The Wake Low in a Midlatitude Mesoscale Convective System Having Complex Convective Organization

GREGORY J. STUMPF* AND RICHARD H. JOHNSON

Department of Atmospheric Science, Colorado State University, Fort Collins, Colorado

BRADLEY F. SMULL

Mesoscale Research Division, National Severe Storms Laboratory, Boulder, Colorado

(Manuscript received 18 October 1989, in final form 26 April 1990)

ABSTRACT

An analysis has been carried out of the surface pressure field in a highly complex mesoscale convective system that occurred on 3–4 June 1985 during the Oklahoma–Kansas Preliminary Regional Experiment for STORM-Central (OK PRE-STORM). During its mature stage the storm consisted of two primary intersecting convective bands approximately 200 km in length, one oriented NE–SW (to the north) and the other N–S (to the south), with a stratiform precipitation region extending to the northwest of the bands. Stratiform precipitation was weak to nonexistent in the southernmost portion of the storm.

Although the organization of the storm was complex, the surface pressure field resembled those associated with simpler, quasi-linear squall systems containing trailing stratiform regions: a mesohigh existed near the convective line and a wake low was observed to the rear of the stratiform region. A strong system-relative, descending rear inflow jet was observed in the northern part of the storm near the wake low. Significantly, only the northern portion of the storm had a trailing stratiform region and it was only in that region that a wake low and a descending rear inflow jet occurred.

An analysis of dual-Doppler radar data taken in the northern part of the storm indicates remarkably strong, localized subsidence at low levels within the rear inflow jet, up to 6 m s^{-1} on a 10-km scale at the back edge of the trailing stratiform region. The maximum sinking occurred (a) to the rear of the highest reflectivity portion of the trailing stratiform region, (b) within the region of the strongest low-level reflectivity gradient, and (c) was coincident with the strongest surface pressure gradient [up to 2 mb (5 km)$^{-1}$] ahead of the wake low center.

These findings indicate that the trailing stratiform precipitation regions of mesoscale convective systems can be dynamically significant phenomena, generating rapidly descending inflow jets at their back edges and, consequently, producing pronounced lower-tropospheric warming, intense surface pressure gradients and strong low-level winds.

1. Introduction

Commonly, the surface pressure field associated with a mature squall line (as described by Fujita 1955; and Pedgley 1962) consists of a mesohigh centered just to the rear of the leading convective line and, farther to the rear, a trailing wake low. In addition, a presquall mesolow is often observed ahead of the leading convective line (Hoxit et al. 1976). This overall pattern is typical for squall lines possessing a stratiform cloud system to the rear of the leading convective line. In many instances, however, stratiform precipitation areas may be found preceding or straddling the convective elements (e.g., Newton and Fankhauser 1964; and Newton 1966) or may trail only a portion of the convective line (Houze et al. 1989; Houze et al. 1990). The position of the surface mesohigh is again typically found in the vicinity of the deep convective cores; however, the expected positions of surface mesolows in these cases are less well-understood.

It is generally held that subsidence is the mechanism responsible for surface mesolows in the vicinity of mesoscale convective systems (Fritsch and Chappell 1980, p. 745). In the case of the presquall mesolow, the subsidence occurs in the mid to upper troposphere and appears to be a compensation for strong upward motion in the leading convective line (Fankhauser 1974; Hoxit et al. 1976; Gamache and Houze 1982). For squall lines with trailing stratiform cloud systems, there also appears to be a region of subsidence that produces a warm lower troposphere just to the rear of the stratiform rain area which, hydrostatically, accounts for the wake low there (Williams 1963; Zipser 1977). Johnson and Hamilton (1988) and Zhang and Gao

* Present affiliation: Cooperative Institute for Mesoscale Meteorology Studies, University of Oklahoma, Norman, OK 73019.

Corresponding author address: Dr. Richard Johnson, Department of Atmospheric Science, Colorado State University, Fort Collins, CO 80523.

(1989) have shown that the subsidence producing the wake low occurs within a descending rear inflow jet (Smull and Houze 1985, 1987b) that is commonly observed to the rear of squall lines having trailing stratiform precipitation regions. The observations presented in Pedgley (1962), Zipser (1977), Johnson and Hamilton (1988), Bosart and Seimon (1988), Johnson et al. (1989), Brandes (1990), Leary and Bals (1989), and Fortune (1989) and the modeling studies of Zhang et al. (1989) and Zhang and Gao (1989) indicate a close link between the stratiform precipitation region and wake lows. One of the goals of this study is to further explore this linkage and shed new light on the process of wake low formation. Another objective is to examine the nature and causes of wake lows in mesoscale convective systems having asymmetric precipitation structures (Houze et al. 1990), i.e., those which have convective organization considerably more complex than that for squall lines possessing symmetric trailing stratiform precipitation regions.

Considering the lack of understanding of surface pressure features (particularly mesolow formation) in mesoscale convective systems having complex organization, it is our intention to examine such features using data from an experiment that was designed to document just these aspects of mesoscale convective systems [the Oklahoma–Kansas Preliminary Regional Experiment for STORM-Central (OK PRE-STORM)]. A storm that occurred on 3–4 June 1985 over Kansas and Oklahoma has been selected, which initially consisted of a somewhat random cellular structure and later consolidated into two intersecting convective bands (Smull and Augustine 1989). The aspect of this system which makes it particularly valuable for the study of mesolow formation and its relationship to stratiform precipitation is the existence, in the mature stage of the storm, of a pronounced north–south variation in the amount of stratiform cloud cover and precipitation.

This paper is closely related to two others, by Leary and Bals (1989) and Green (1989), that also deal with the mesoscale convective systems that occurred on 3–4 June. Using dual-Doppler radar data, Leary and Bals (1989) have investigated the surface pressure field and its relationship to the stratiform precipitation region, as done here, but on a scale larger than that reported in this study. Green (1989) has examined the surface pressure field accompanying the convective system studied here and two others that occurred in the succession of storms on 3–4 June. These papers provide a broad framework within which the results of our study can be viewed.

2. Data and analysis procedures

a. PRE-STORM conventional observations

A complete description of the OK PRE-STORM observational systems and networks can be found in Cunning (1986). In this study considerable emphasis was given to data from the National Center for Atmospheric Research (NCAR) Portable Automated Mesonetwork (PAM II) and National Severe Storms Laboratory Surface Automated Mesonetwork (NSSL SAM) surface measurement systems. In particular, reliable documentation of the mesohighs and mesolows accompanying this storm requires 1 to 2 mb accuracy of the pressure sensors. Johnson and Toth (1986) have conducted an analysis of the PAM data that indicates that this required accuracy has been readily achieved in PRE-STORM (an approximate 0.5 mb absolute accuracy for the PAM data, following corrections). Considering that the primary mesoscale pressure perturbations associated with the storm passed through the PAM mesonet (in Kansas and northern Oklahoma), these features should be very well described by this dataset.

In order to remove topographic effects from the pressure analyses, the pressures have been adjusted hydrostatically to the mean elevation of all stations, 480 m MSL, using the surface virtual temperature as an approximation to the mean virtual temperature for the column. The use of the surface value is required since sounding data do not exist to give the true virtual temperature lapse rate above each station. Possible errors created by this procedure are estimated to be <0.5 mb. Additionally, two other modifications to the pressure data have been made: 1) atmospheric tidal effects have been removed based on the mean diurnal pressure variations for five of the PAM stations during May and June, and 2) corrections for instrument bias have been made using a procedure described in Stumpf (1988). The resulting pressure adjustments are similar, though not identical, to those presented in Johnson and Hamilton (1988).

The upper-air data consist of 90-min soundings from National Weather Service (NWS) sites and twelve supplemental sites and nearly continuous observations from three 50-MHz wind profiling systems at Liberal, Kansas; McPherson, Kansas; and Norman, Oklahoma.

Satellite data are from GOES West, a United States geostationary satellite situated at 105°W during the experiment. Conventional radar observations have been merged into composite displays using digitized NWS WSR-57 10-cm radars located at Amarillo, Texas; Oklahoma City, Oklahoma; Garden City, Kansas; Wichita, Kansas; and Monett, Missouri.

b. Dual-Doppler radar data

To explore details of the precipitation and airflow structure associated with the wake low, a dual-Doppler analysis has been performed at 0107 UTC 4 June using data from the NCAR CP-3 and CP-4 5-cm Doppler radars, which were located along a 60 km baseline in southcentral Kansas (Fig. 1). Three additional dual-Doppler volumes (0037, 0051, and 0059 UTC) have also been analyzed over a 30-min period ending at 0107

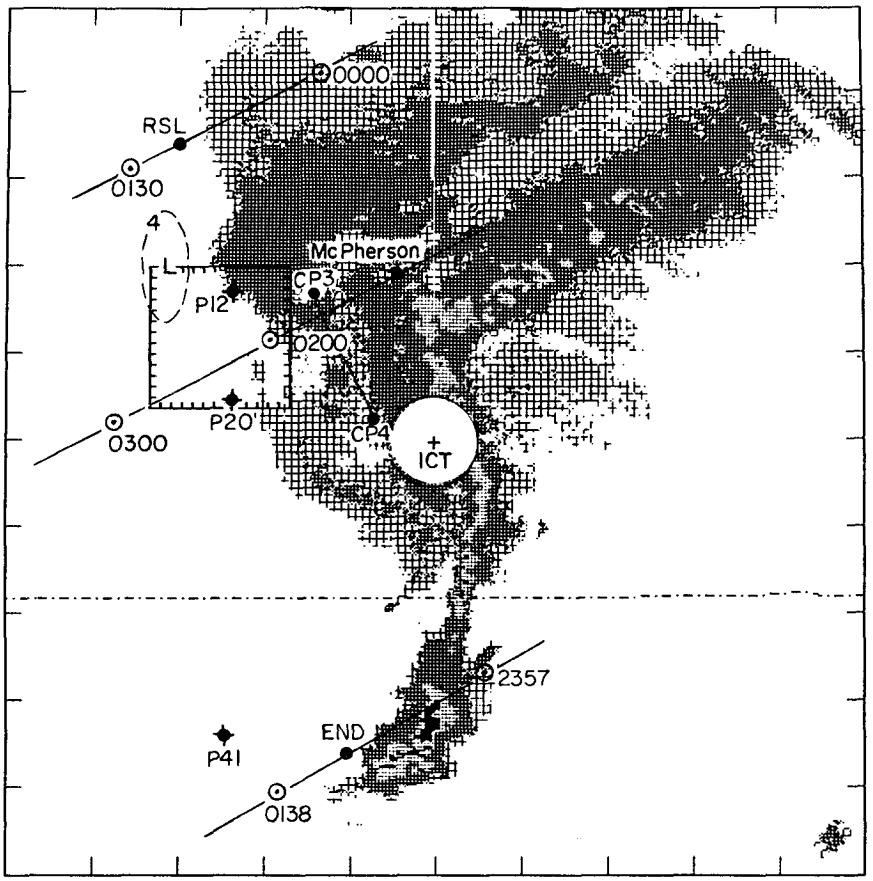

FIG. 1. Radar reflectivity (shading representing <25, 25–43, 44–50, >50 dBZ) at 0105 UTC, 4 June 1985, from WSR-57 radar at Wichita, KS (ICT). NCAR CP-3 and CP-4 dual-Doppler analysis domain (65 km × 65 km box) is positioned at back edge of trailing stratiform precipitation region. Innermost closed isobar (954 mb) near the surface or 480 m MSL around wake-low center (L) is indicated. Also shown are positions of NCAR PAM Stations 12, 20, and 41; sounding sites at Russell, KS, (RSL) and Enid, Oklahoma (END); and wind profiler site at McPherson, Kansas. Storm-relative positions of individual soundings are indicated using an estimated stratiform-back-edge motion of 240° at 18 m s^{-1}. Tick marks on outer perimeter are at 40-km intervals.

UTC. All show features very similar to the 0107 UTC analysis, but are not presented here for two reasons. First, the 0051 and 0059 UTC volumes were not intended for dual-Doppler synthesis, but rather for EVAD (Extended Velocity Azimuth Display; Srivastava et al. 1986) analysis. This mode of data collection appreciably degrades vertical resolution at lower levels far from the radars where the main features of interest were located. Second, at 0037 UTC, when data were truly collected in a coordinated dual-Doppler fashion, the primary area of study was located near the fringe of reliable vector winds. Encouragingly, results from an independent dual-Doppler analysis at 0037 UTC by Leary and Bals (1989) also support many of the present analysis of the 0107 UTC volume. Details of the radar characteristics and scanning strategies of CP-3 and CP-4 are provided in Rutledge et al. (1988). findings from present analysis of the 0107 UTC volume. Details of the radar characteristics and scanning strategies of CP-3 and CP-4 are provided in Rutledge et al. (1988). Data for this time are also presented by Smull and Augustine (1989); however, the present analysis focuses on the wake-low region and, thus, encompasses a different part of the storm.

Horizontal winds and reflectivity were objectively analyzed at 1-km intervals in the horizontal and vertical between 0.5–15.5 km AGL. The horizontal winds were subjected to a low-pass filter, effectively eliminating horizontal wavelengths less than 10 km. Vertical velocities were determined from downward integration of the anelastic continuity equation, subject to the constraint of vanishing vertical motion at the upper and lower boundaries.[1] All winds displayed are system-relative, using a motion of 18 m s^{-1} from 240° appro-

[1] All heights referenced in conjunction with the Doppler radar analysis are above ground level with respect to the CP-4 radar, which was located at an elevation of 438 m MSL. Refer to Smull and Augustine (1989) for a summary of Doppler analysis procedures.

priate to the storm's trailing edge (as explained in the next subsection). The analysis covers a 65 km × 65 km area (Fig. 1) that straddles the back edge of the surface rainfall region. Its northern boundary passes close to the center of the wake low; extension of the analysis farther to the north was precluded by error considerations related to the geometry of the PRE-STORM Doppler network. However, the specified domain allows one to contrast structure in the vicinity of the wake low with conditions to its south, where a much weaker pressure perturbation was observed. Additionally, comparisons of measurements from the surface mesonetwork to lower-tropospheric processes revealed by Doppler radar can be sought.

c. *Determination of system motion*

The mesoscale convective system on 3–4 June had a very complex structure and pattern of motion. To aid in understanding this structure, the circulation within the system will be depicted in many of the subsequent analyses in a framework relative to the motion of the storm itself. Since the primary focus of this study is on the wake low, a storm motion appropriate for this phenomenon was determined by examining the direction and speed of motion of three features: the rear edge of the surface stratiform rain, the axis of maximum stratiform rain rate, and the surface meso-high axis, all determined from PAM data. The movement of the wake low axis itself was not used since it turned out to be a far less conservative feature and exhibited some erratic behavior. Details of these analyses can be found in Stumpf (1988).

The average motion of the three features described above is 18 m s^{-1} from 240° (±3 m s^{-1}/5°). This estimated motion is similar to the 18 m s^{-1}/230° values used by Leary and Bals (1989) in their dual-Doppler analysis of this storm. Sounding data from three stations, Russell (RSL) and McPherson, Kansas, and Enid (END), Oklahoma, will later be displayed in time series during the storm's passage. The system-relative positions of these observations, using a time-to-space conversion based on the above motion, are indicated in Fig. 1. The McPherson profiler time series projects through the dual-Doppler analysis region and provides a useful comparison with the Doppler-derived winds. The system-relative positions of the 2357 and 0138 END soundings may be somewhat in error since certain features of the echo pattern (e.g., the southernmost intense convective cell) in Oklahoma exhibited motion more nearly from 270°. A portion of this echo contained a tornadic supercell, which propagated to the right of the mean flow. Nevertheless, other features such as the leading edge and southern tip of the N–S line tracked more closely to the estimated wake-low features, and, therefore, 18 m s^{-1}/240° was used for all system-relative motion displays.

3. Synoptic overview

The mesoscale convective system (MCS) under study was the second of four that traversed the Oklahoma–Kansas region on 3–5 June 1985 (Augustine and Howard 1988). Each was separated by approximately eight hours and all were sufficiently large and long-lived to be classified as Mesoscale Convective Complexes (MCCs), after Maddox (1980). The first three followed very similar tracks, as has been observed in other instances of multiple MCS development (Fritsch et al. 1986). The development of the second MCS was undoubtedly influenced by the first, particularly through the effects of a surface outflow to the rear of the first system. The aim of this overview is to present enough of the synoptic and regional-scale setting for the second MCS to provide a proper framework for discussion of its wake-low development.

a. *Surface and upper-air features*

All four MCSs developed in the vicinity of a warm frontal boundary, which extended from northern Oklahoma to the northern Texas Panhandle. At 1200 (all times UTC) on the morning of 3 June this front emanated from a low in the Texas Panhandle (Fig. 2). The initial convective cells for the first MCS developed in southern Kansas (× in Fig. 2) approximately 100 km to the north of the surface frontal position, with a later expansion of the convection and movement to the northeast. The location of the initial development

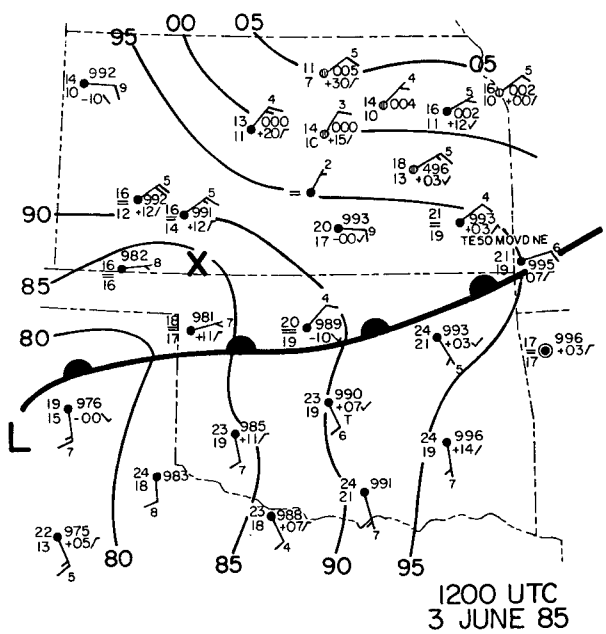

FIG. 2. Surface pressure (altimeter settings; e.g., 90 = 29.90 in Hg) analysis at 1200 UTC 3 June 1985. × marks the location of the formation of the first radar echo (at 1300 UTC) for the first mesoscale convective system in the series on 3–4 June.

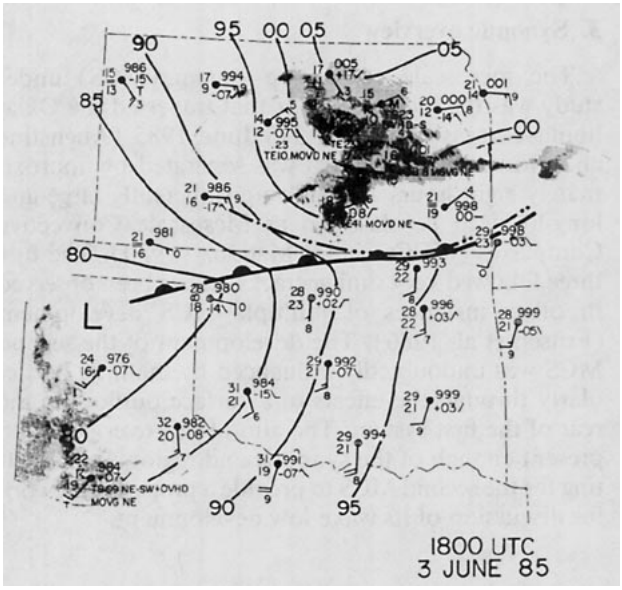

FIG. 3. As in Fig. 2, except at 1800 UTC and with Amarillo, Texas, and Wichita, Kansas, radar echoes (15, 25, 35, and 50 dBZ) included. Double-dot dashed line indicates outflow boundary.

of this system presented a severe challenge for forecasters since no obvious surface triggering mechanism existed in this warm front overrunning situation (Stumpf and Johnson 1988).

Over the next six hours the first MCS developed, matured, and began its decay with the dissipating remnants occupying the northeast portion of Kansas at 1800 (Fig. 3). At this time a cold outflow extended to the south and west of the radar echoes in this region, and this air served to enhance a quasi-stationary east–west front along the Kansas–Oklahoma border. PAM and SAM data have been used to define the frontal position and outflow boundary in Fig. 3.

The formative storms for the second MCS are seen to be entering the Texas Panhandle as a broken north–south line at 1800 (Fig. 3). The initial cells for this system were first observed in extreme southeastern New Mexico. The subsequent track and surface pressure features associated with this system will be discussed later using mesonetwork data.

The flow at 500 mb at 1200 UTC 3 June was characterized by a slowly eastward moving cutoff low over the southwestern United States (Fig. 4). Weak positive vorticity advection by the thermal wind was seen to be entering the PRE-STORM area at this time, which may have provided some lifting to help initiate the MCSs. The nearly quasi-stationary nature of the large-scale flow field and surface frontal boundary in the region likely contributed to the recurrence of MCSs along similar tracks in the PRE-STORM area. These tracks were generally along an anticyclonic path curving to the northeast, as prescribed by the 500-mb flow (Fig. 4).

b. Satellite and radar images

A sequence of satellite pictures at approximately 2-h intervals from 1800 to 0430 is shown in Fig. 5. The second MCS in the series is seen in Fig. 5 to develop in the Texas Panhandle at 1800 (a), expand and enter western Oklahoma and Kansas at 2000 (b), and pass through the central and eastern portion of the PRE-STORM region during its mature phase between 2200 and 0230 (c–e). Finally, at 0430 (f), the storm dissipated as it passed into Missouri.

A sequence of WSR-57 radar composites for this time period is presented in Fig. 6. At 1800 and 2000 (Figs. 6a,b) the storm system is comprised of somewhat banded, although largely disorganized convective elements over the Texas Panhandle. Little attendant stratiform precipitation is evident at these times. Two

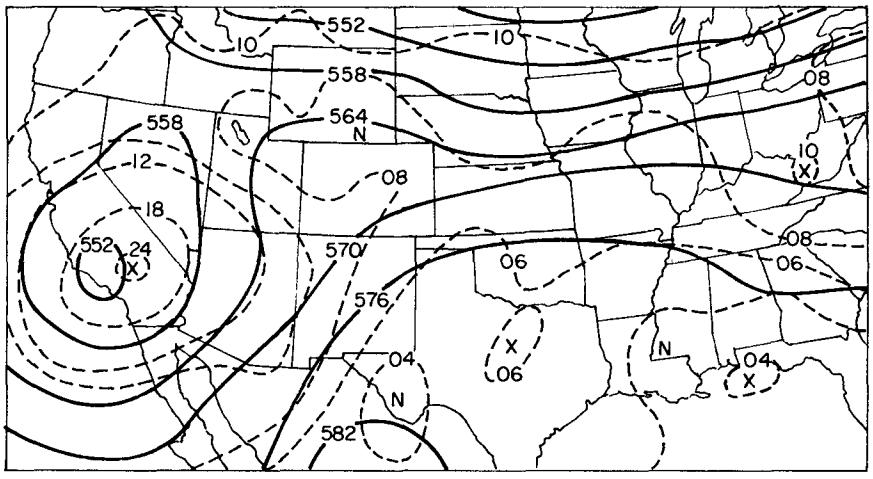

FIG. 4. 1000–500 mb thickness lines in dm (solid) and absolute vorticity in 10^{-5} s^{-1} (dashed) at 1200 UTC 3 June 1985.

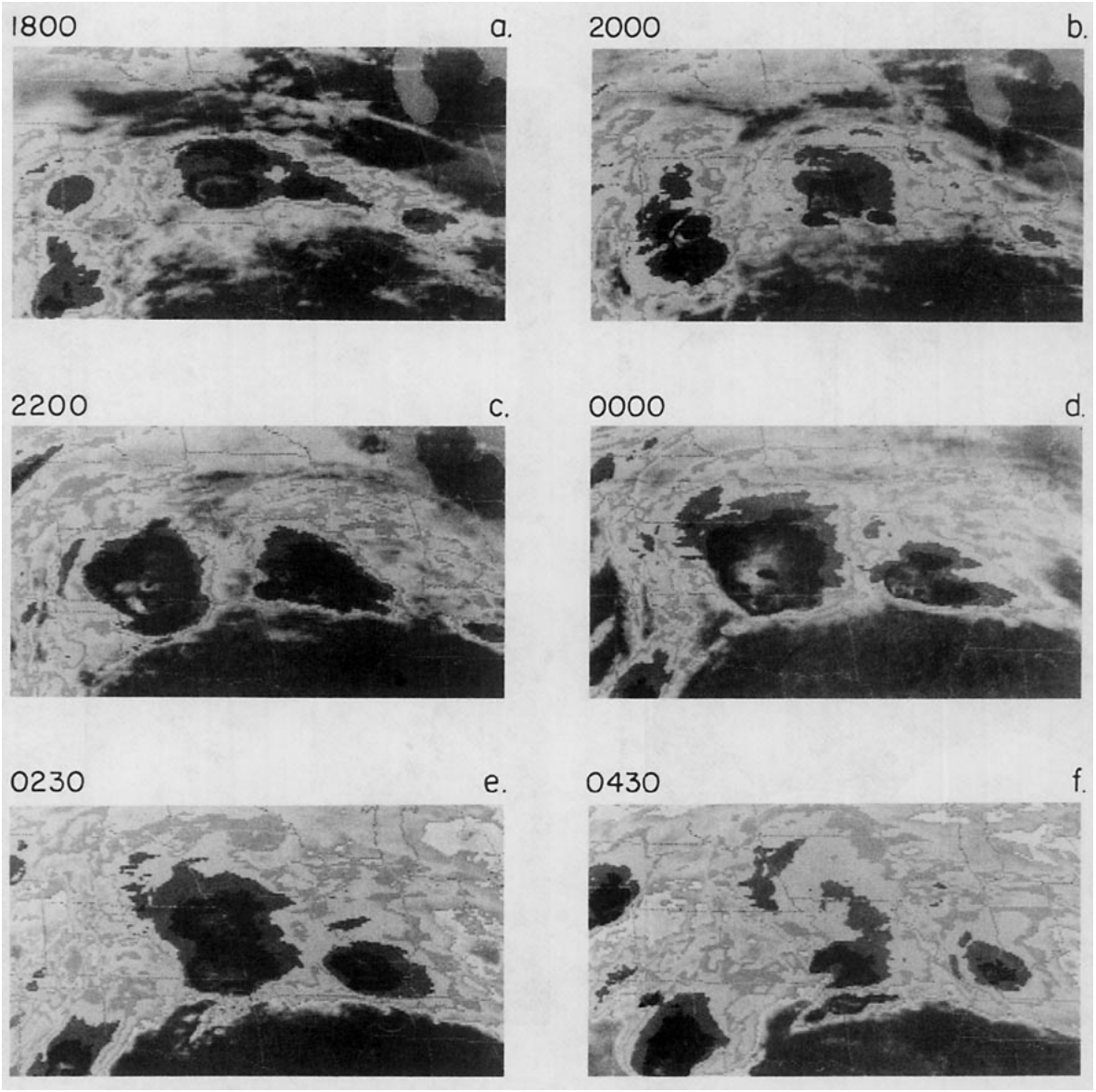

FIG. 5. Infrared satellite pictures at 1800, 2000, and 2200 UTC 3 June (a)–(c) and 0000, 0230, and 0430 UTC 4 June 1985 (d)–(f).

hours later, at 2200 (c), an expansion and eastward propagation occurs with a greater degree of organization into lines and an increase in associated stratiform precipitation. The convective band extending eastward just south of the Kansas–Oklahoma border is positioned along the east–west warm front in that location (Fig. 3).

Considerable changes in the storm structure occurred within the next two hours. By 0010 (Fig. 6d) the loosely-organized convective bands and elements consolidated into one continuous structure characterized by 1) an intense, N–S convective line at the southern end with no associated stratiform precipitation (the portion of the line containing a tornadic supercell indicated by T); and 2) a poorly-organized, NE–SW band or region of deep convection with an extensive area of stratiform precipitation extending to the west and north. At this mature stage of the MCS, the overall precipitation structure resembles an "open wave" or developing cyclone on the synoptic scale, as pointed out by Smull and Augustine (1989), although the time and space scales for the MCS are considerably shorter than those for synoptic-scale systems and the surface pressure fields do not mimic an open wave cyclone. The transition of this MCS from a chaotic to more organized structure relatively late in its lifetime stands in contrast to that of squall lines, which tend to take on linear organization at a relatively early stage and maintain it over long periods of time. Analysis of single-Doppler radar data near this time by Smull and Au-

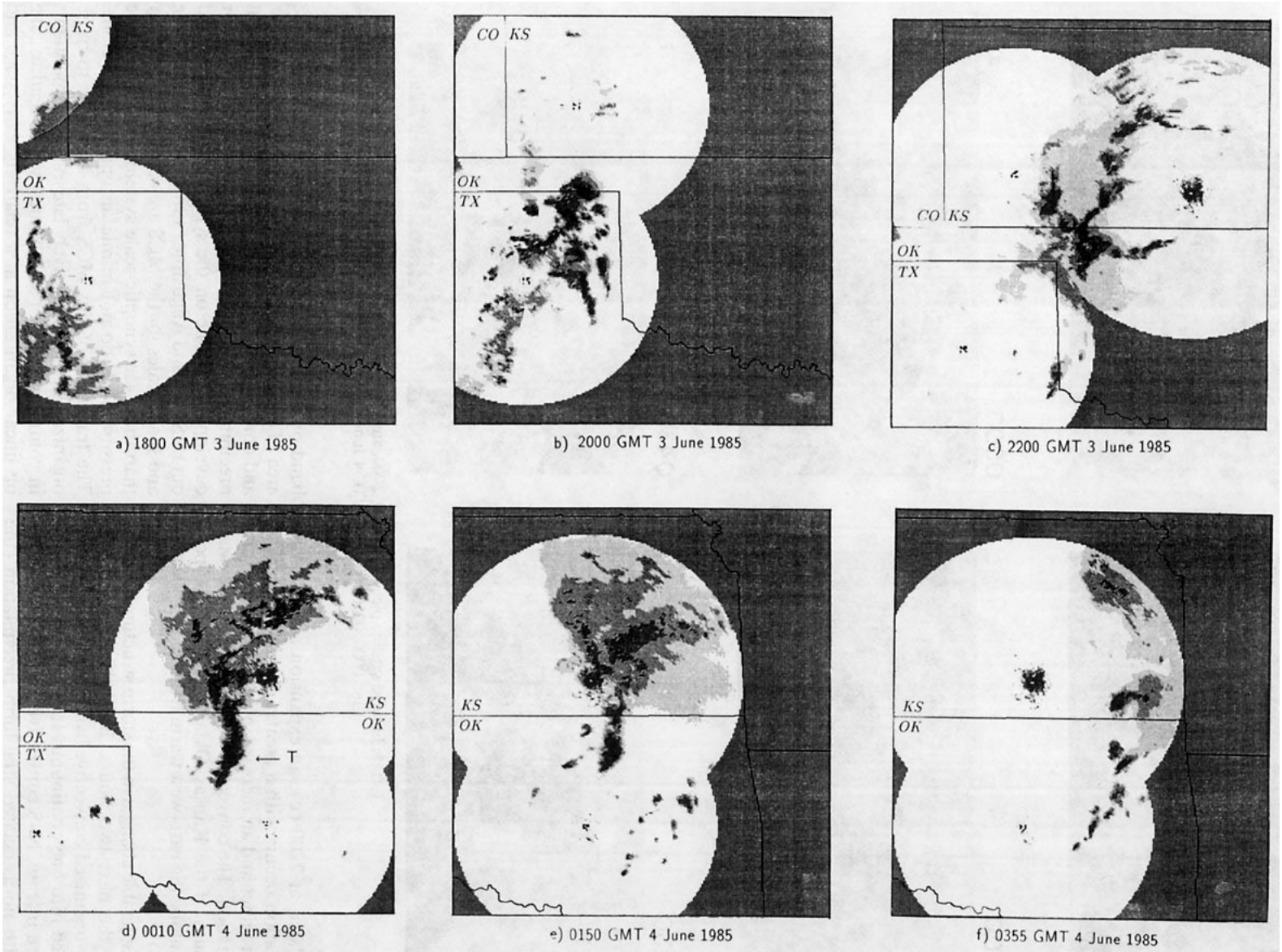

FIG. 6. Composite radar reflectivity (values exceeding 15, 25, 35, and 50 dBZ indicated by successively darker shading) at 1800, 2000, and 2200 UTC 3 June (a)–(c) and 0010, 0150, and 0355 UTC 4 June 1985 (d)–(f). T in (d) indicates position of tornadic supercell.

gustine (1989) indicates that the most intense deep convection existed in the southern line where updrafts were rooted in more unstable boundary layer air to the south (Fig. 3). Convection in the northern region was weaker, with broader updrafts, and cellular convective structure was suppressed. The convective development in the northern region occurred above a cool, stable air mass that existed at the surface to the north of the warm front. Smull and Augustine attribute the contrasting south to north convective structure to the presence of the frontal zone in this region and outflow (cool, stable air) from the first MCS.

The lack of significant attendant stratiform precipitation in the southern portion of the N–S line is largely a consequence of an absence of any pronounced system-relative flow at upper levels normal to it (a sounding time series at Enid, Oklahoma, will be presented later to illustrate this feature; Fig. 13). The majority of the hydrometeors at upper levels in the southern part of the N–S line were therefore advected predominantly along it into the northern portion of the MCS.

This open wave structure was to some degree preserved over the next 2-h period (Fig. 6e). However, by 0150 (e) some weakening of the southern line and eastward expansion of the stratiform precipitation was observed. During the next two hours, further weakening occurred, and the MCS exited the PRE-STORM region by 0355 (f) in its dissipating stage.

4. Mesoanalysis of wake low

Despite the rather complex precipitation structure of this MCS, it still contained mesoscale surface pressure features that closely resemble those for squall lines with trailing stratiform regions: a presquall mesolow, a mesohigh, and a wake low. However, as will be shown, the wake low in this case appeared in only a portion of the trailing region of the MCS.

At 2000 (Fig. 7a) the first MCS in the series is seen to be departing the northeast portion of the mesonetwork. The back edge of a mesohigh and a weak wake low or trough are observed at the dissipating phase of this system at this time. The surface outflow from this system extends through the wake low and far enough south to meet up with the warm front (Fig. 3). This boundary is therefore indicated as an outflow boundary in Fig. 7a. The second MCS is entering the western portion of the mesonetwork and appears to have associated with it a presquall mesolow. However, this low may to a large extent be a manifestation of the subsynoptic low present in this region at an earlier time (Fig. 3).

Two hours later, at 2200 (Fig. 7b), the convection has entered west-central Kansas and western Oklahoma with a wind-shift line or gust front at its leading edge and a mesohigh to the west, very likely associated with the rain-cooled air in this region. The mesohigh is strongest in the region of expanding convection in Kansas. An eastward movement of the mesolow in Oklahoma is also evident, although the relationship of this low to convection in this region is probably somewhat obscured by the existence of a semipermanent low or pressure trough in the western part of that state (Fig. 3). One hour later at 2300 (not shown) the Kansas mesohigh moved entirely into the mesonetwork and the first evidence of a developing wake low appeared along the western edge of the stratiform region.

At 0020 the mesohigh and wake low in Kansas have both intensified significantly and a strong pressure gradient between the two has developed (Fig. 7c). The axis of the wake low in Kansas is along the back edge of the trailing stratiform precipitation (also noted and studied by Leary and Bals 1989). The mesohigh is centered within the heavy precipitation region in Kansas, and a lobe of high pressure extends along the squall line into Oklahoma. However, the mesohigh is far less intense along the narrow convective band in this region than it is in Kansas. Moreover, there is no well-defined wake low in this southern segment and the front-to-rear pressure gradient is considerably weaker.

Further intensification of the pressure gradient between the mesohigh and wake low in the northern part of the mesonetwork occurred over the next hour such that by 0120 (Fig. 7d) the pressure gradient reached its peak value. The wake-low center and zone of strongest pressure gradient occurred adjacent to the highest reflectivity portion (exceeding 35 dBZ) of the trailing stratiform region.

The pressure drop associated with the passage of the wake low is illustrated in a time series (Fig. 8) of surface observations for P12, the station near the center of the wake low in Fig. 7d. Following the passage of the mesohigh, a drop in pressure of 6 mb in 30 min was observed around 0100. The rate of fall over the final 5 min of this 30-min period, from 0105 to 0110, reached a remarkable 2.2 mb (5 min)$^{-1}$. This rapid fall is similar to the 8 mb (20 min)$^{-1}$ drop that was recorded in the vicinity of a trailing stratiform region during the 28 May PRE-STORM squall event (S. A. Rutledge, personal communication). Even more rapid falls than these, 9 mb (20 min)$^{-1}$, have been reported in two other squall lines by Williams (1954) and Bosart and Seimon (1988). As in our case, the rapid falls in each of these other storms occurred at the rear edge of the surface stratiform precipitation region trailing a leading convective line.

The time series in Fig. 8 shows that the rapid pressure fall occurred during a storm-ending period of lighter (stratiform) rainfall, averaging 6 mm h^{-1}, from 0040 to 0110. The rapid pressure fall terminated around the time of cessation of stratiform rain. This sequence is consistent with the results reported by Williams (1954), Fujita (1955), Pedgley (1962) and in the 10–11 June PRE-STORM case by Johnson and Hamilton (1988). In the present study there were actually two episodes (of approximately 80-min duration) of heavy rainfall

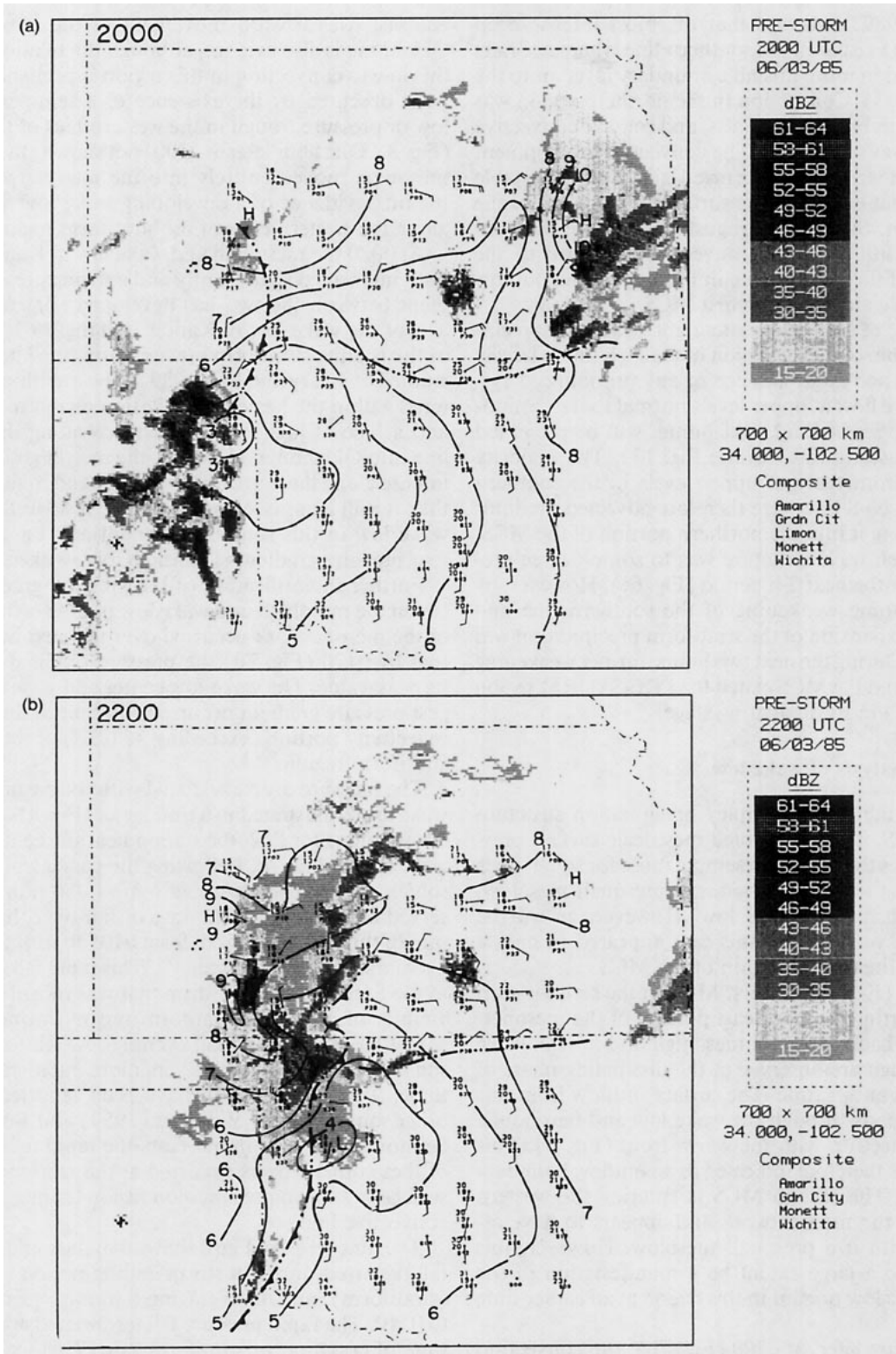

FIG. 7. Surface mesoanalysis, including isobars for 480 m MSL-adjusted pressure (e.g., 6 = 956 mb) and radar reflectivity (scale on right) for 2000 and 2200 UTC 3 June (a) and (b). 0020, 0120, and 0300 4 June 1985 (c)–(e).

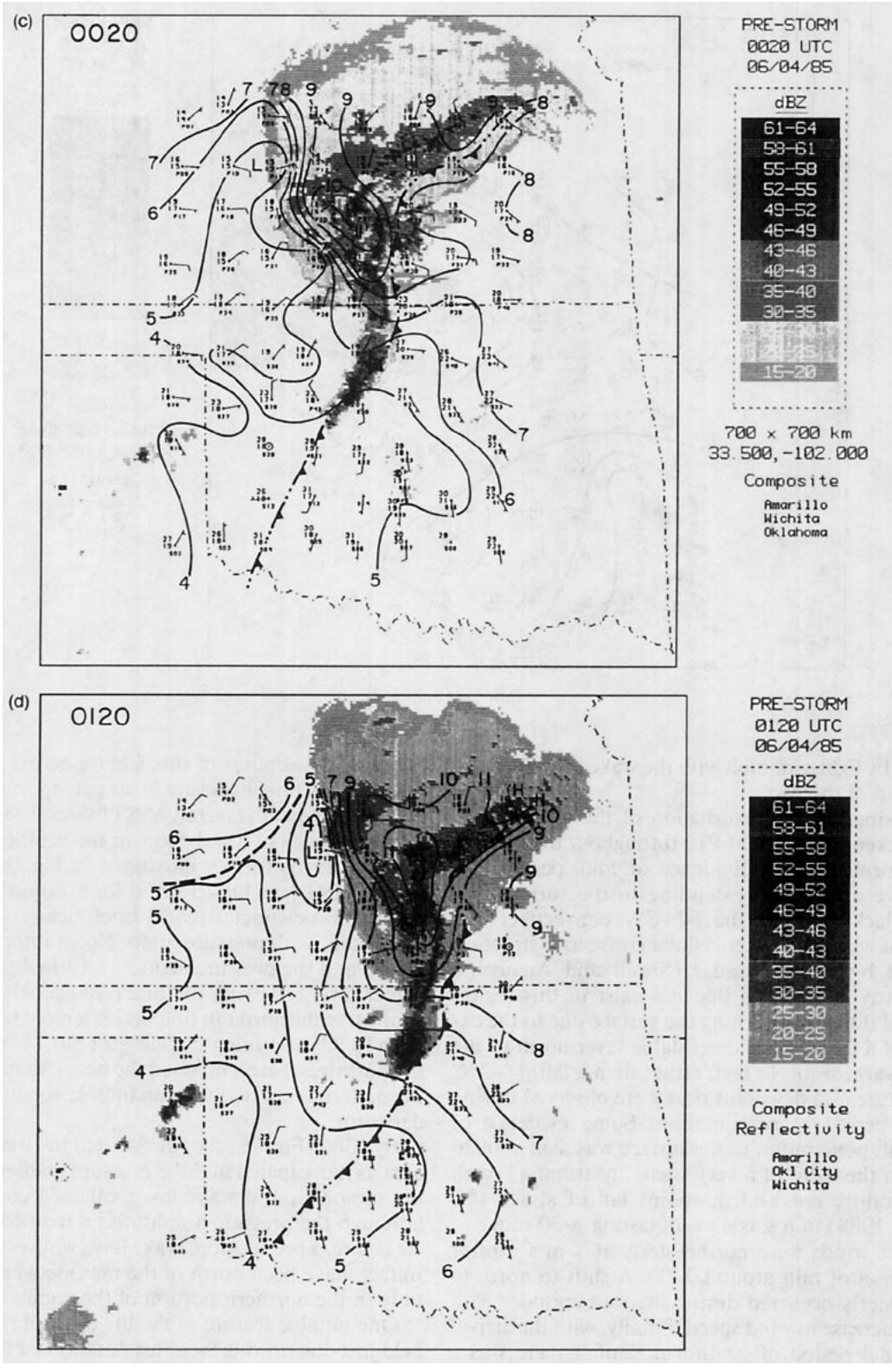

FIG. 7. (*Continued*)

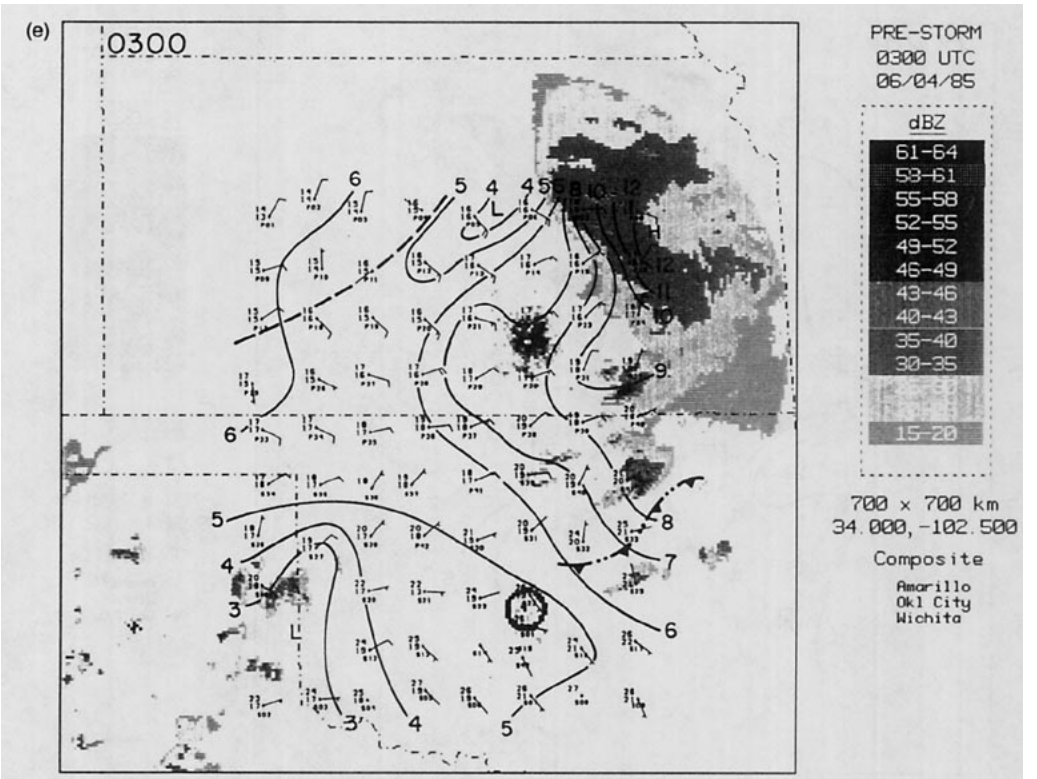

FIG. 7. (*Continued*)

followed by lighter rainfall with the wake low following the second of the two.

Surprisingly little perturbation of the temperature and dewpoint occurred at P12 throughout the passage of the storm (Fig. 8). Evidence of cold, penetrating convective downdrafts extending to the surface was notably lacking along the NE–SW convective line, consistent with the weaker cellular convective structure indicated by Doppler radar (Smull and Augustine 1989). Any downdrafts that did exist in this region likely had difficulty reaching the surface due to the existence of a 0.5–1.0 km deep stable layer north of the surface warm front. In fact, rather than a fall, 1°–2°C temperature and dewpoint rises were observed during the 2-h period of precipitation. Some evidence of downdraft penetration to the surface was seen at 0020 at P19 in the form of a very weak "heat burst," with a temperature rise and dewpoint fall of about 1°C (Stumpf 1988) in a single event lasting ~30 min.

Surface winds were northeasterly at 5 m s^{-1} prior to the onset of rain around 2200. A shift to north to northwesterly occurred during the rain episodes with a slight increase in wind speed. Finally, with the arrival of the final period of stratiform rainfall there was a return to an easterly flow with a gust to 15 m s^{-1} at 0110, the time of the cessation of the rapid pressure fall. Although a sudden easterly acceleration of the flow occurred while P12 was in the strong east–west pressure gradient, extreme velocities did not develop because of the rapid translation of this feature across the region and the only brief exposure of air parcels to the intense pressure gradient (Garratt and Physick 1983).

The absence of a wake low in the southern portion of the storm is further illustrated in Fig. 9 by a time series at P41 (see Figs. 1 or 7d for position). The line passage was characterized by brief, heavy rain and an associated 3-mb pressure jump. No stratiform rain occurred and the pressure actually returned to a slightly higher level following the line passage. Also in sharp contrast to the northern time series, a rapid temperature drop (8°C) and intense wind gust (to 24 m s^{-1} from the northwest) accompanied the heavy rain, much like the patterns expected with an intense squall-line thunderstorm.

By 0300 (Fig. 7e) the MCS exited the mesonetwork area as it dissipated and the pressure gradient between the mesohigh and wake low weakened considerably, although the pressure amplitudes remained the same. As before, a pronounced wake low (whose center may, in fact, have been north of the mesonetwork) appears only in the northern portion of the region.

One notable feature of the life cycle of the pressure field just described is the short duration (several hours) of an extreme pressure gradient between the mesohigh and wake low. This pressure gradient builds up to a maximum amplitude in our case near 0130 and then gradually weakens. Both in this case (Fig. 7d) and in two others already studied (Johnson and Hamilton

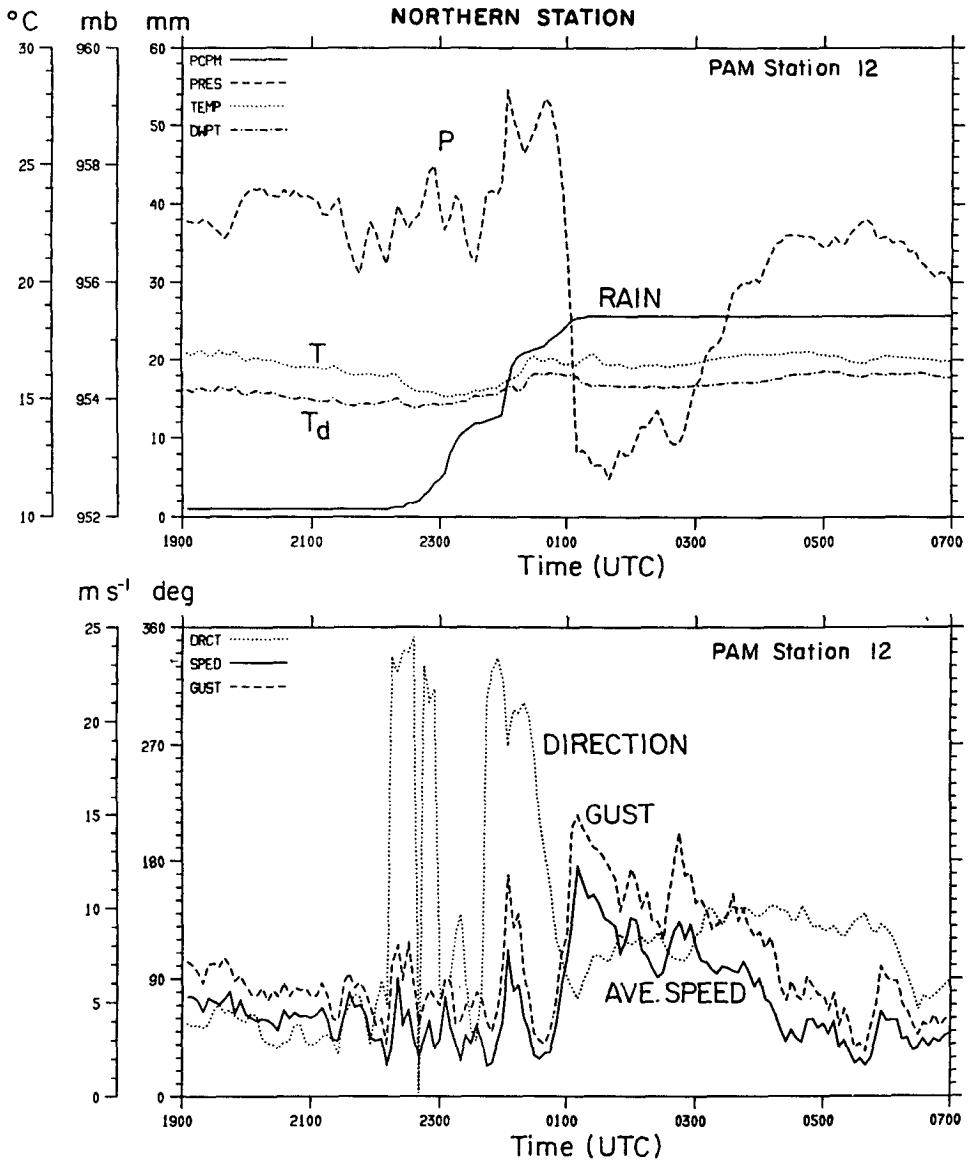

FIG. 8. Time series of station pressure (mb), accumulated rainfall (mm), temperature (°C), dewpoint (°C), and wind direction, speed, and peak gust (m s^{-1}) for NCAR PAM Station 12 (position indicated in Fig. 1) for 3–4 June 1985.

1988; Johnson et al. 1989) the maximum pressure gradient occurs within and at the time of maximum reflectivity gradient at the back edge of the trailing stratiform region. This relationship will be displayed more precisely using dual-Doppler radar data in section 6.

Despite significant differences in the mature convective structure and evolution of this MCS and linear squall systems, the surface pressure features at 0020 and 0120 (Figs. 7c,d), at least over Kansas, resemble those for a maturing to mature squall line (e.g., the 10–11 June PRE-STORM squall line; Johnson and Hamilton 1988). Namely, a presquall trough, squall mesohigh and developing wake low (hugging the back edge of the trailing stratiform region) are all features reported during the mature phase of the highly linear system studied by Johnson and Hamilton (1988). These features are not so convincingly present, however, in the southern portion of the MCS where little to no stratiform precipitation exists.

This contrast suggests that there may be a direct correspondence between the existence of a trailing stratiform region and the existence of an associated wake low. Such a correspondence was suggested by Johnson and Hamilton (1988) in the study of a squall line wherein they found a direct correlation between the intensity of wake lows and the intensity of trailing

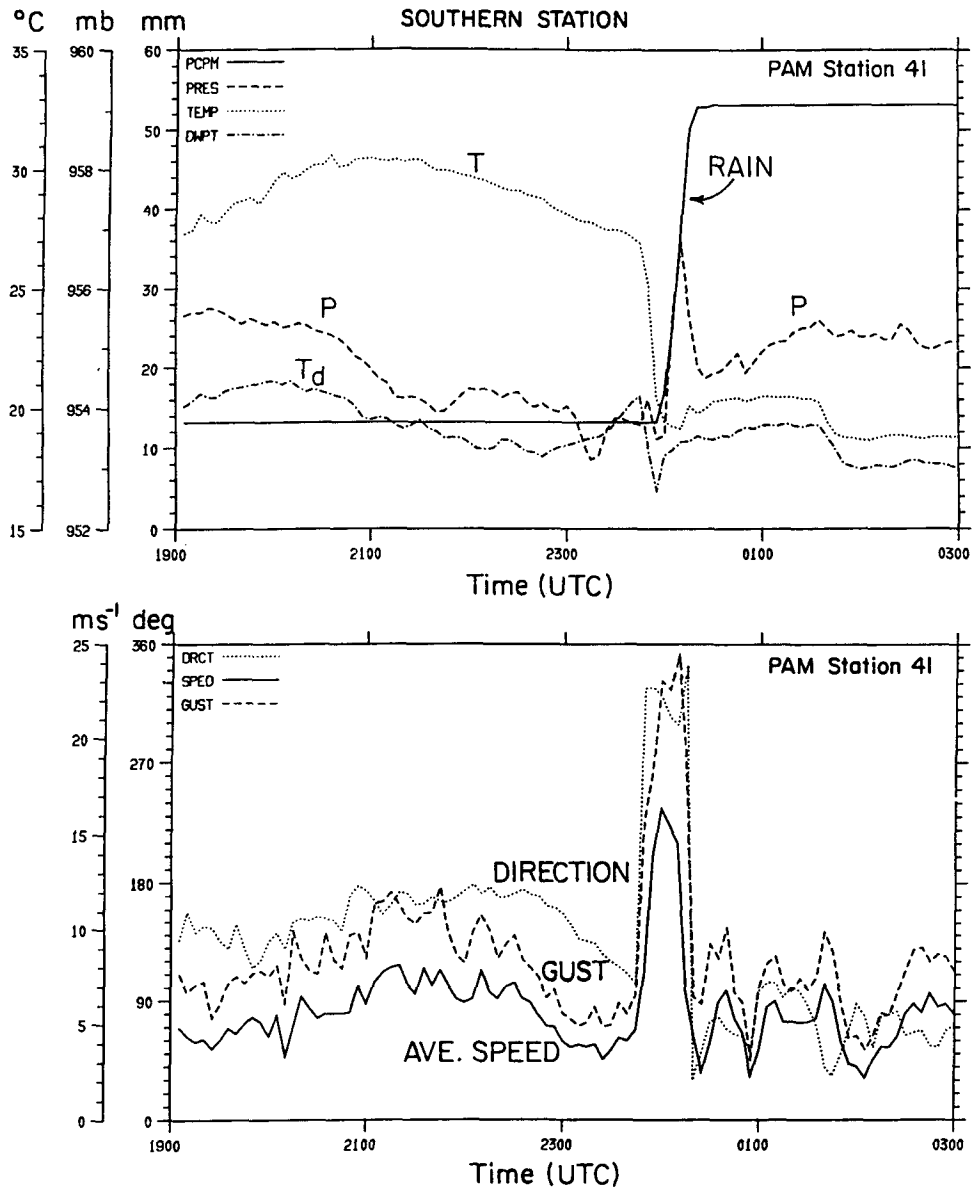

FIG. 9. As in Fig. 8, except for PAM Station 41.

stratiform precipitation. The absence of a wake low to the rear of the southern convective line suggests that mechanisms associated with stratiform precipitation may be essential to the production of a wake low. Further discussion of this matter will be given later.

5. Tropospheric wind and thermodynamic structure in north and south portions of the MCS

In order to explore possible causes of north-to-south variations in the surface pressure field behind the storm, time series of sounding data from three stations are examined (Russell, Kansas, McPherson, Kansas, and Enid, Oklahoma). System-relative distances represented by these time series are indicated Fig. 1. The Russell and McPherson sections represent the structure for the northern part of the storm in the vicinity of the wake low (although neither passes directly through the low center), while the Enid section represents the structure for the southern portion, which has no wake low. Since the storm was far from steady, these time sections do not accurately represent its spatial structure; however, they do provide an indication of important physical processes around the time of rainfall termination at the back edge of the storm.

The time series for Russell, Kansas, (Fig. 10) shows a pronounced rear inflow jet, locally exceeding 15 m s^{-1}, entering the trailing stratiform rain region just be-

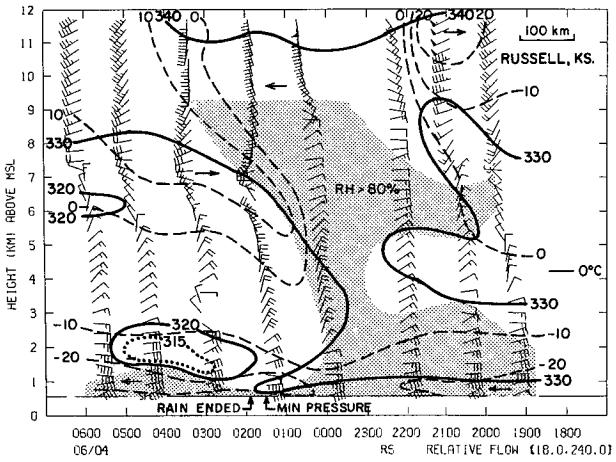

FIG. 10. Time–height cross section of system-relative winds (one half barb = 2.5 m s^{-1}; one full barb = 5.0 m s^{-1}; one flag = 25.0 m s^{-1}), equivalent potential temperature (K; solid contours at 10 K intervals, selected intermediate contours are dotted), and isotachs for component of wind in plane of section (m s^{-1}, dashed) at Russell, KS, from 1800 UTC 3 June to 0600 UTC 4 June 1985. Relative humidity greater than 80% (with respect to ice at temperatures below 0°C) is shaded.

low the upper-level cloud base (inferred from sounding relative humidity data to be near 6–8 km). This flow configuration is, in part, similar to that determined for the trailing stratiform regions of midlatitude squall lines studied by Smull and Houze (1985, 1987a, 1987b) and Rutledge et al. (1988), and illustrated in the conceptual model of Houze et al. (1989). However, an important difference between this case and the others cited is the apparent failure, evident in the RSL time series and the dual-Doppler analysis to follow in section 6, of the rear inflow jet to extend through the stratiform rain region toward the leading convective line. The dual-Doppler radar data show the rear inflow in this part of the storm, rather, to descend rapidly to low levels at the back edge of the stratiform rain region and feed into the outflow behind the system near the ground. This particular behavior may have been important in generating intense surface pressure and reflectivity gradients at the back edge of the trailing stratiform region, as will be discussed later.

The "flaring" (strongly backing with height) character of the winds in this jet over Russell (top left to center portion of Fig. 10) also resembles that determined from wind profiler data within the rear inflow jet of the 10–11 June PRE-STORM squall line (Augustine and Zipser 1987). This structure can also be seen with greater time resolution from wind profiler time series from McPherson (Fig. 11). The half-hourly observations from this site indicate a descent of this jet to as low as 3 km at 0200, approximately 20 minutes after the cessation of surface rainfall there.

The 0130 sounding at Russell, taken near the time of minimum pressure in the wake low, shows the effects of strong descent with pronounced warming and drying in the lower troposphere (Fig. 12). From 0000 to 0130 there is an increase in the mean virtual temperature from the surface to 500 mb of 2.7 K. The hydrostatic surface pressure change corresponding to this warming (computed from Eq. (2) of Johnson, et al. 1989) is −4.0 mb. This change agrees reasonably well, though is slightly larger than a fall of 3.5 mb observed between 0000 and 0130 at the Russell sounding site. Apparently, some cooling above 500 mb is compensating the low-level warming at Russell (Fig. 12). This finding supports the studies of Williams (1963), Zipser (1977), Johnson and Hamilton (1988), and Johnson et al. (1989), all of which indicate subsidence warming in the lower troposphere as the mechanism for wake low production.

An additional mechanism potential contributing to the pressure variation could be the change in hydrometeor loading across the sharp back edge of the stratiform region. Using radar reflectivity–water mass relationships in Leary and Houze (1979), the maximum pressure fall associated with this effect is estimated to be 0.4 mb. It is concluded that water loading variations across the back edge of the stratiform region provide a very minor contribution to the production of the wake low.

At Russell at 0130, two dry layers are actually present, as opposed to just one commonly seen at low levels to the rear of squall lines (the latter referred to as an "onion" sounding by Zipser 1977[2]). In this instance (Fig. 12), the sounding is far enough to the rear of the storm to separately penetrate the low-level warm, dry, rearward-directed flow from the lower-tropospheric branch of the descending rear inflow jet, giving the lower onion structure, and the forward-flowing mid-tropospheric branch of the jet, giving the upper dry layer.

One noteworthy feature of the Russell time series (Fig. 10) is the existence of very low values of θ_e centered near 1.5 km AGL to the rear of the stratiform region. These values are at least 5 K lower than any observed in the midtroposphere either to the front or rear of the storm.

One possible explanation for this feature is the horizontal transport of low θ_e air into the region behind the storm. Unfortunately, Russell is on the northern periphery of the supplemental sounding sites and lower-tropospheric data immediately north of the site are not available. However, examination of 0000 sounding data from all surrounding stations shows higher values of θ_e than those at Russell in the lower troposphere, suggesting that some process other than horizontal transport may be responsible for this feature. Such a process might be the vertical transport of low θ_e values

[2] Actually, several of the cases summarized by Zipser (1977) and displayed in Smull and Houze (1987b) show evidence of the double "onion" structure we see here.

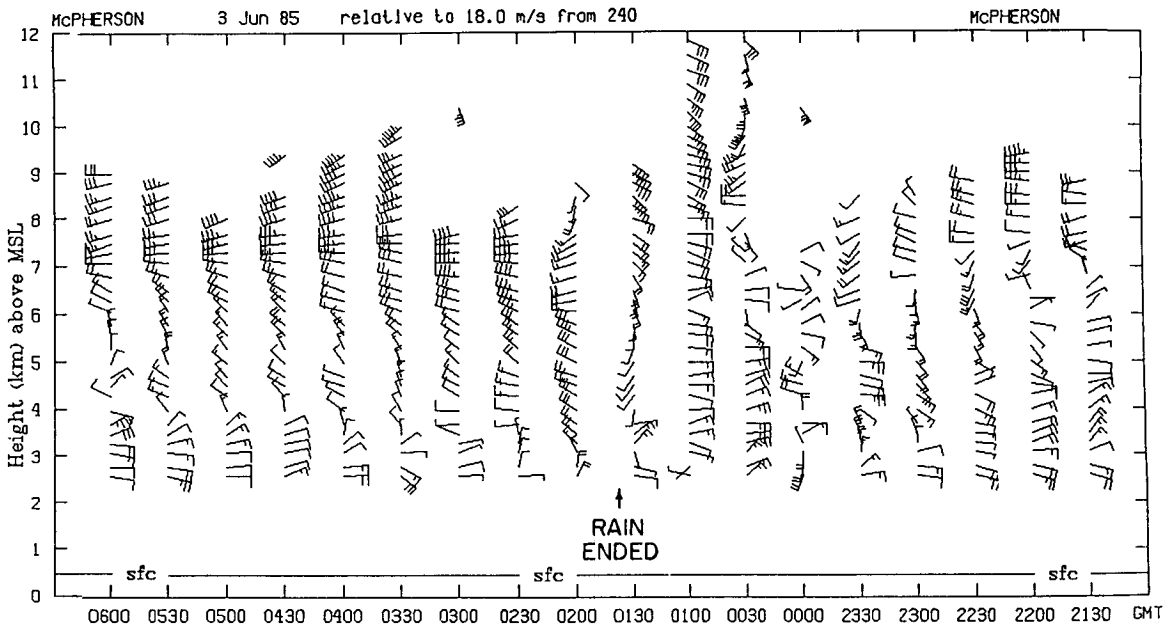

FIG. 11. Time–height section of winds (as in Fig. 10) from wind profiler at McPherson, Kansas, from 2130 UTC 3 June to 0600 UTC 4 June 1985.

from a midtropospheric minimum in the surrounding region lower than that observed at Russell. However, information on such a minimum is not available.

Yet another plausible explanation could involve vertical transport plus the nonconservative effects of sublimation and/or melting (since θ_e is defined in terms of the latent heat of vaporization). Leary and Houze (1979) and Smull and Houze (1987b) have shown that considerable cooling can be realized due to melting of precipitation within the stratiform region. An estimate of 3 K cooling by melting at the back edge of a 1976 Oklahoma squall line was determined by Smull and Houze (1987b) based on an assumed 40-km length of trajectory of the flow in the melting layer. This value is similar to the reduction in θ_e we observe. A similar calculation was attempted for this case, but the non-steadiness of the line, the three-dimensionality of the flow and the lack of data have precluded an accurate determination of the trajectories of air associated with the θ_e minimum. One is forced to conclude that the data do not permit a satisfactory explanation for the low θ_e area found behind the storm at this time, although any one or a combination of the above factors may have been responsible.

The time series at Enid, Oklahoma, across the southern part of the storm shows a sharply contrasting relative flow and thermodynamic structure to its rear (Fig. 13). Although system-relative rear inflow is also observed near the base of an upper-level anvil cloud (which is thinner in this case), it does not penetrate significantly toward the surface at the back edge of the line. Consistent with this lack of a strong descending rear inflow jet is the absence of a significant reduction in θ_e in the lower troposphere behind the line. The lack of a pronounced descending rear inflow is also evident from the 0138 Enid sounding (Fig. 14), which shows little net change in temperature and dewpoint above the boundary layer from the 2357 presquall sounding (which appears to have been ingested in the leading

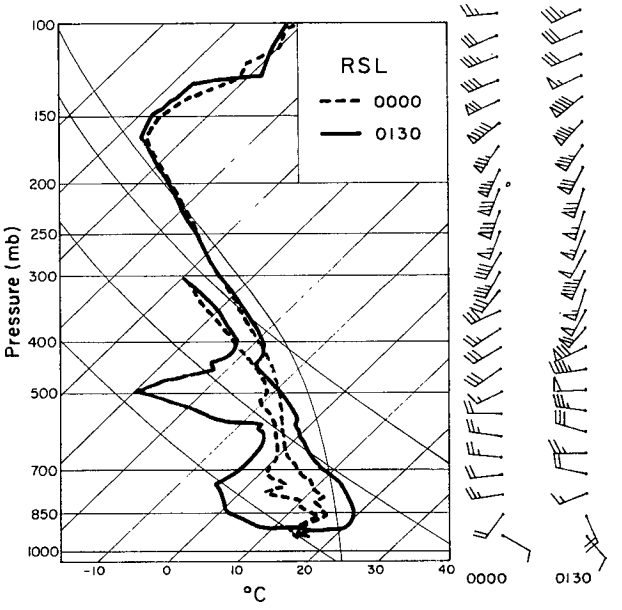

FIG. 12. Skew-T plots of temperature and dewpoint at Russell, Kansas, at 0000 (dashed) and 0130 (solid) UTC 4 June 1985.

convective line). The absence of low-level warming behind the southern portion of the storm is also consistent with the lack of a wake low there (Figs. 7c,d and 9).

In summary, a pronounced descending rear inflow jet and warm, dry lower troposphere are observed in the vicinity of the wake low in the northern part of the storm. In the southern part, a descending rear inflow jet and warm, dry lower troposphere are not observed, and neither is a wake low. The presence of an extensive stratiform region in the north and virtually none in the south suggests that a trailing stratiform cloud is essential to the production of a wake low. This conclusion was also suggested from the analysis of the 10–11 June PRE-STORM squall line wherein it was determined that a splitting of the wake low into two parts accompanied a corresponding splitting of the trailing stratiform region (Johnson and Hamilton 1988).

6. Lower-tropospheric processes contributing to the wake low

a. Dual-Doppler radar analysis

Figure 15 presents the system-relative airflow and radar reflectivity over the rear of the storm at a height of 1.5 km AGL, along with the near-surface (480 m MSL) pressure for the analysis domain in Fig. 1. The echo pattern is clearly stratiform in character, but exhibits a sizable reflectivity gradient along its back edge. This gradient is especially sharp in the vicinity of the wake low ($y > 45$ km in Fig. 15). [A large trailing-edge reflectivity gradient was also noted in association with an intense wake low in the 28 May (S. A. Rutledge, personal communication) and 24 June (Johnson et al. 1989) PRE-STORM squall events.] As mentioned previously, the low developed adjacent to a region of relatively intense stratiform rainfall, whose southern

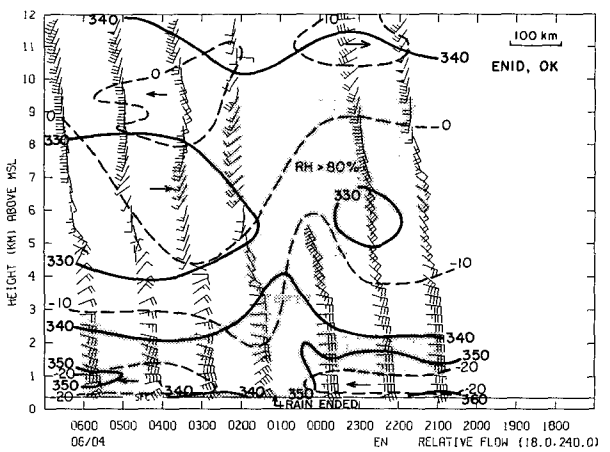

FIG. 13. As in Fig. 10, except for Enid, Oklahoma.

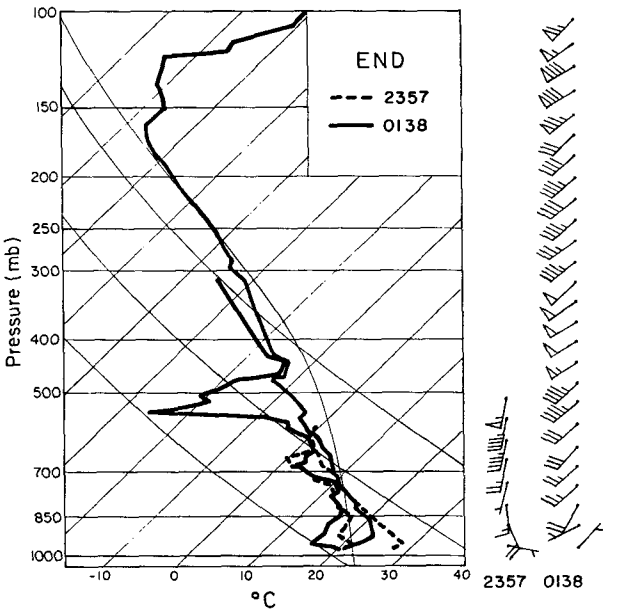

FIG. 14. Skew-T plots of temperature and dewpoint at Enid, Oklahoma, at 2357 UTC 3 June (dashed) and 0138 UTC 4 June (solid) 1985.

edge corresponds to reflectivity values exceeding 35 dBZ. The surface pressure gradient[3] is a maximum immediately adjacent to and on the precipitating side of the strongest reflectivity gradient. To the south the reflectivity and surface pressure gradients are both much weaker.

System-relative winds at 1.5 km (Fig. 15) are from the northeast and basically unidirectional, but pronounced speed divergence is depicted in the northern reaches of the domain. This evidently corresponds to acceleration of air toward the wake low; peak speeds in this zone approach 45 m s^{-1} (25 m s^{-1} from the northeast in the ground-relative frame). A similar acceleration of the surface wind at station P12 occurred in this zone, corresponding to the period of most rapid pressure fall (cf., Fig. 8). At the time of the Doppler analysis P12 was located along the track of the center of the wake low at $(x, y) = (-66$ km, 60 km), as shown in Fig. 15. Much less acceleration of the low-level flow is evident in the southern part of the domain, i.e., away from the wake-low center, in the vicinity of P20 at $(x, y) = (-66$ km, 8 km). The relationship of

[3] The pressure analysis is based on data from 5-min observations at P12 and P20 at the northern and southern portions of the domain. Because of the coarseness of the surface data on this small scale, the reliability of the analysis between stations is somewhat limited. The pressure gradients in the north and south portion are, however, felt to be tenable. An analysis similar to that displayed in Fig. 15 (0.5 h earlier and on a somewhat larger scale) has been presented by Leary and Bals (1989).

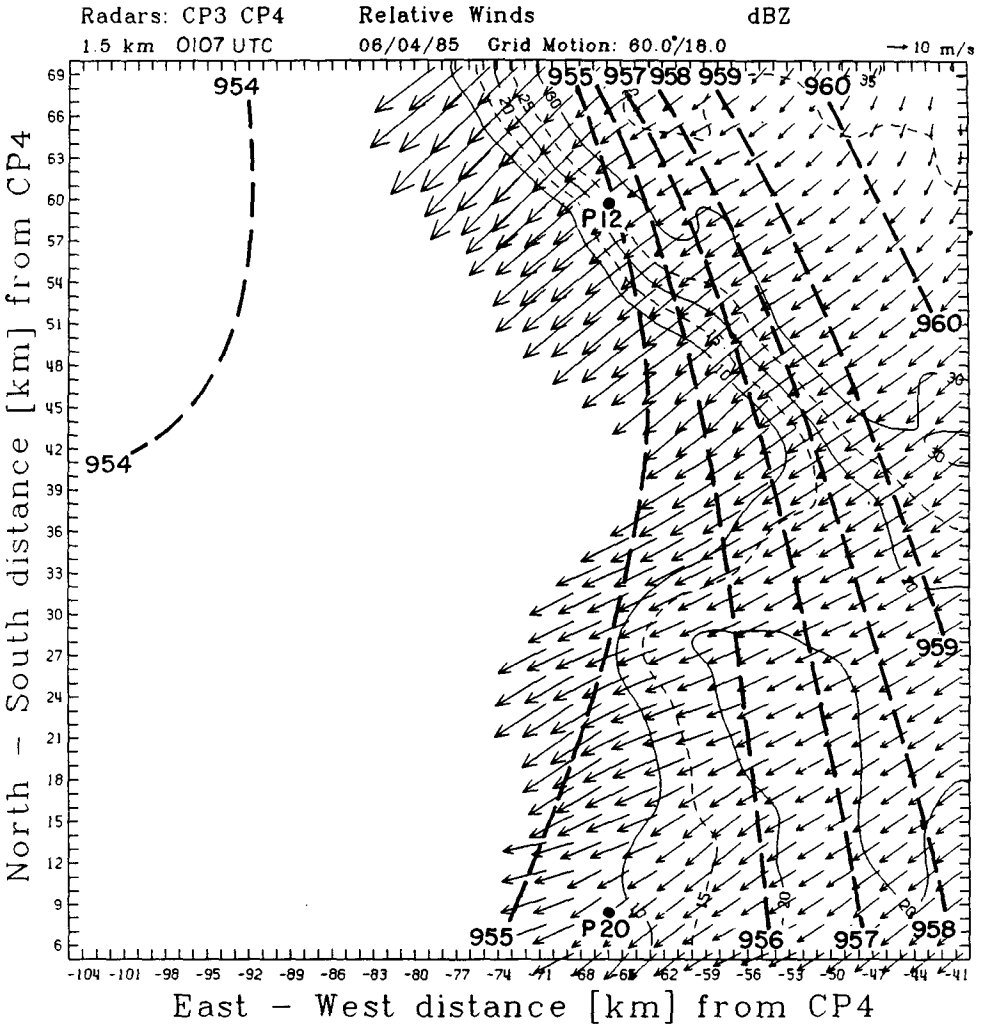

FIG. 15. Radar reflectivity (light contours, dBZ) for wake-low domain (Fig. 1), dual-Doppler derived system-relative winds (m s^{-1}, scale at upper right) and 480 m MSL-adjusted pressure (bold dashed contours, mb) at 1.5 km AGL at 0107 UTC 4 June 1985. PAM Stations 12 and 20 are indicated.

these surface data to the radar-derived storm structure will be discussed in more detail later in this section.

Flow was extremely perturbed in the lower to mid-troposphere over the wake-low region, as illustrated by the 3.5-km analysis (Fig. 16). The sharp reflectivity gradient found near the surface remains apparent, but at these levels is associated with strongly convergent flow resulting from interaction of northwesterly relative winds behind the storm with easterly-component flow in the stratiform rain region. [This convergent interface is also apparent in a dual-Doppler analysis of this system at 0037 UTC discussed by Leary and Bals (1989).] The convergence is accompanied by cyclonic vorticity, which is even more pronounced at the 4.5–5.5 km levels (not shown). However, this circulation was apparently confined to small scales, as no significant midlevel vorticity was resolved by the PRE-STORM rawinsonde network (Stumpf 1988; Smull and Augustine 1989).

With increasing distance away (i.e., south) from the wake-low center, the reflectivity gradient relaxes and the wind field takes on a much smoother appearance. Although the gradient region continues to exhibit slight cyclonic vorticity, the marked convergence detected near the center of the wake low is no longer evident, as westerly flow penetrates farther into the stratiform echo.

The significance of the profoundly disturbed horizontal winds near the wake low is further illustrated by vertical cross sections in that vicinity. Figure 17 displays an east–west section along $y = 60$ km (oriented approximately perpendicular to the back edge of the stratiform rain area). This section passes directly over surface station P12, which was located within the intense reflectivity gradient zone at the time of the analysis. Selected data from the time series at P12 (cf., Fig. 8) are shown to either side of this location in Fig. 17

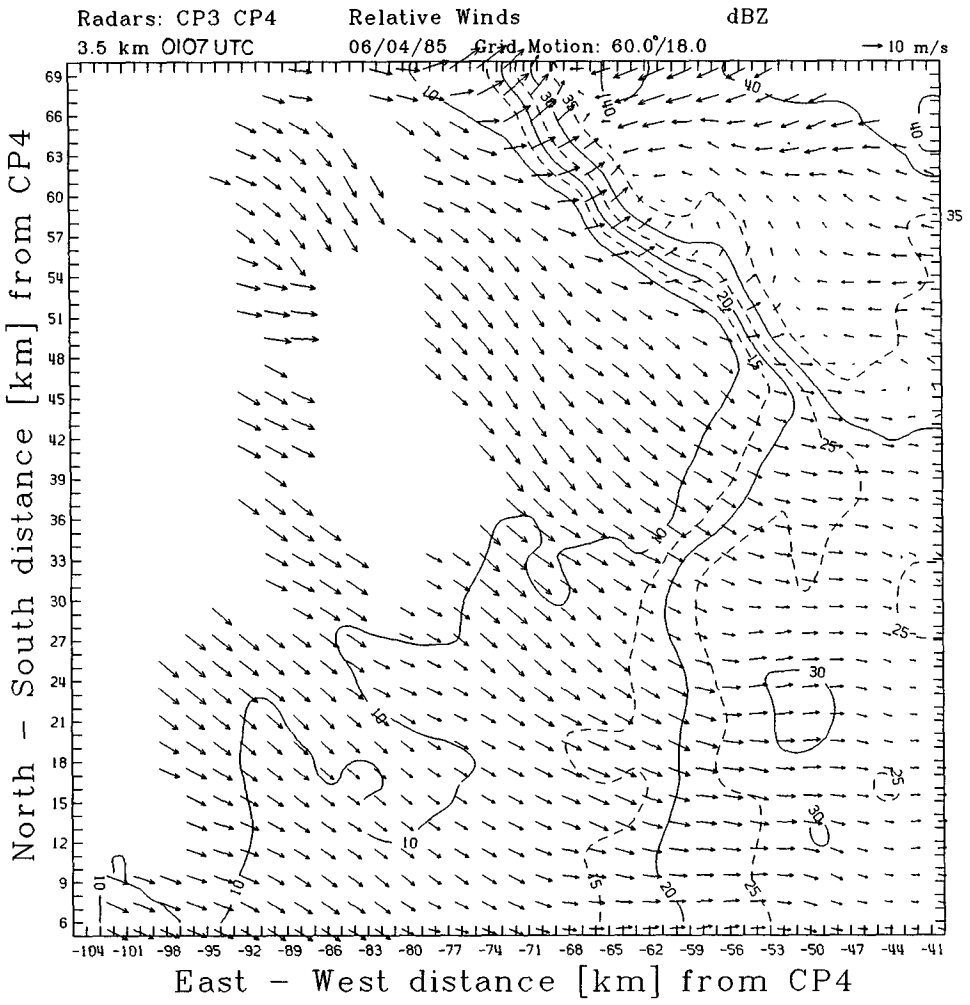

FIG. 16. Radar reflectivity (dBZ) and dual-Doppler derived system-relative winds (m s^{-1}) for wake-low domain at 3.5 km AGL at 0107 UTC 4 June 1985.

by applying a time-to-space conversion based on the u component of the trailing edge motion (i.e., eastward at 15.6 m s^{-1}). In this manner, the sequence of events at the surface may be related to processes occurring aloft.

The main features of the reflectivity field include a bright-band maximum (Fig. 17) near the 3.5-km level within the stratiform rain area ($x > -65$ km), while to the west a large echo "overhang" is indicative of evaporation (or at higher levels sublimation) of stratiform precipitation prior to reaching the surface. The velocity pattern is composed of three principal regimes: 1) a deep layer of front-to-rear (i.e., easterly component) relative flow in the upper troposphere responsible for carrying hydrometeors originating in deep convection (located well east and south of the domain; cf., Fig. 1) into the upper reaches of the trailing stratiform region; 2) opposing westerly-component flow impinging upon the system's back edge between 3 and 7 km; and 3) strong easterly flow below 3 km directed toward the wake low. [The relationship of these features to the system's overall structure is described in greater detail by Smull and Augustine (1989).] The dual-Doppler derived wind profile at the back edge of the stratiform region at this time is in good agreement with the 0200 McPherson profiler winds (Fig. 11; see Fig. 1 for projected 0200 McPherson position).

The tightly packed reflectivity contours previously noted in Figs. 15 and 16 appear below 4 km near $x = -70$ km in Fig. 17. However, the cross-sectional view sheds new light on the strongly convergent midlevel flow in this zone and its relationship to the wake low. Vertical velocities in Fig. 17 indicate that this convergence fed strong, localized downdrafts (exceeding 6 m s^{-1}) along the system's back edge. In turn, divergence at the base of these downdrafts was at least partly responsible for accelerating low-level flow toward the wake low. The cross section illustrates that the source of air entering these downdrafts lay principally behind (i.e., to the west of) the storm. Upon encountering the

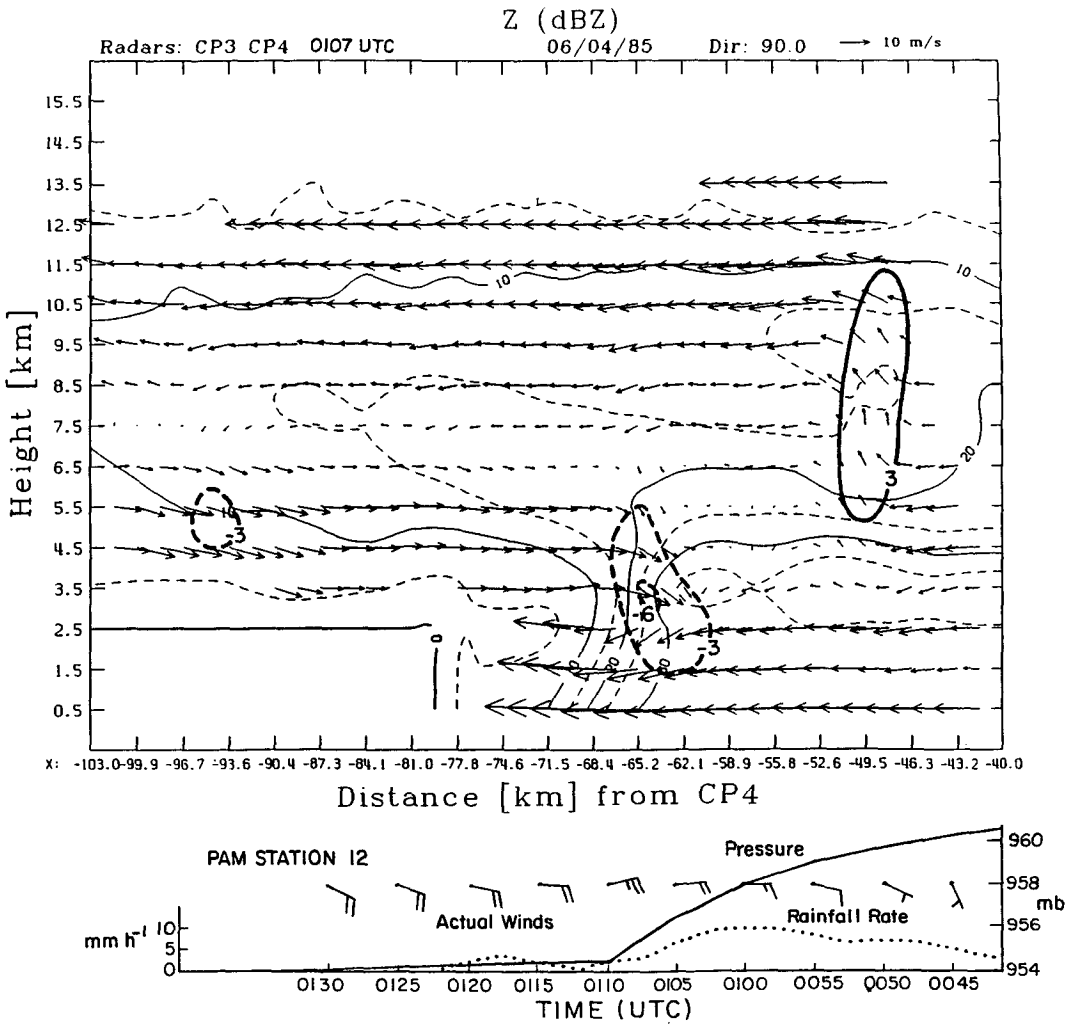

FIG. 17. Vertical cross section of radar reflectivity (dBZ) and dual-Doppler derived system-relative winds (m s^{-1}), 60 km north of CP-4 in the E–W direction across the northern part of wake-low domain (Fig. 1). Vertical motion (3 m s^{-1} intervals) is also indicated. In the lower portion of the diagram time-to-space converted observations of pressure, wind, and rainfall rate at PAM Station 12 are displayed.

"wall" of precipitation constituting the storm's back edge, this dry and potentially cool air (cf., Figs. 10, 12) likely became negatively buoyant and sank rapidly. Evidence for negative buoyancy aloft can be inferred from the 0130 RSL sounding (Fig. 12) where an extremely dry layer exists below 400 mb (7 km). Also, recent dynamic retrieval analyses of perturbation buoyancy in the stratiform cloud (Smull and Jorgensen 1990) confirm the existence of negative buoyancy aloft at 2–3 km AGL.

Thermodynamic data discussed in section 5 (as well as the pressure and rainfall traces at P12 seen in the lower part of Fig. 17) suggest that resultant subsidence warming outweighed the effects of diabatic cooling. In this way, intense downdrafts in the lower troposphere contributed hydrostatically to the rapid pressure decrease observed in this part of the storm. The remarkable correspondence of the downdrafts to the location of most rapid pressure falls (2.2 mb in 5 min or, equivalently, over a distance of 5.4 km) is illustrated by data from surface station P12 shown in Fig. 17. Based on the vertical velocities observed, nonhydrostatic effects could have contributed up to 0.3–0.4 mb of the total pressure change, at most, or less than 10% of the hydrostatic pressure change.

The pronounced low-level warm anomaly to the rear of the stratiform region is a reflection of overshooting of negatively buoyant downdrafts within the descending rear inflow. Deceleration of the downdraft below 3 km (Fig. 17) is consistent with the concept of overshooting and the local production of warm air. The dynamic retrieval analyses of Smull and Jorgensen

(1990) also indicate strong positive buoyancy at low levels (at 1 km) as a result of this overshooting.

Air emerging from the trailing-edge downdrafts combined with flow exiting the stratiform region to produce an exceptionally strong outflow directed to the storm's rear at low levels. The strength of this flow was evidently responsible for the peculiar orientation of reflectivity contours in the vicinity of the mesolow (e.g., between $x = -70$ and -65 km in Fig. 17), which shows that stratiform rain was swept toward the rear as it fell. The peak ground-relative gust of 15 m s^{-1} and 5-min average wind speed of 12.5 m s^{-1} from the east observed as this feature passed over P12 (noted in Figs. 8 and 17) are consistent with this interpretation.

The airflow pattern in Fig. 17 also helps to explain the close correspondence previously noted between the reflectivity and pressure gradient zones in the lower troposphere. The same downdraft warming that was evidently responsible for the precipitous drop in surface pressure also likely served as a strong, localized source of evaporation. In addition, the overlying midlevel convergence constituted the interface between a hydrometeor-rich airstream [flowing rearward across the stratiform region ($x > -60$ km)] and relatively drier air approaching from the west. Together these effects evidently maintained the exceptionally strong reflectivity gradient observed along the stratiform echo's back edge near the wake low.

Much different structure is documented away from the wake-low center. Figure 18 presents a vertical section along $y = 8$ km (passing over station P20, whose pressure and rainfall traces are also shown). It is representative of conditions south of the intense reflectivity gradient zone (i.e., for $y < 45$ km). Absent are the

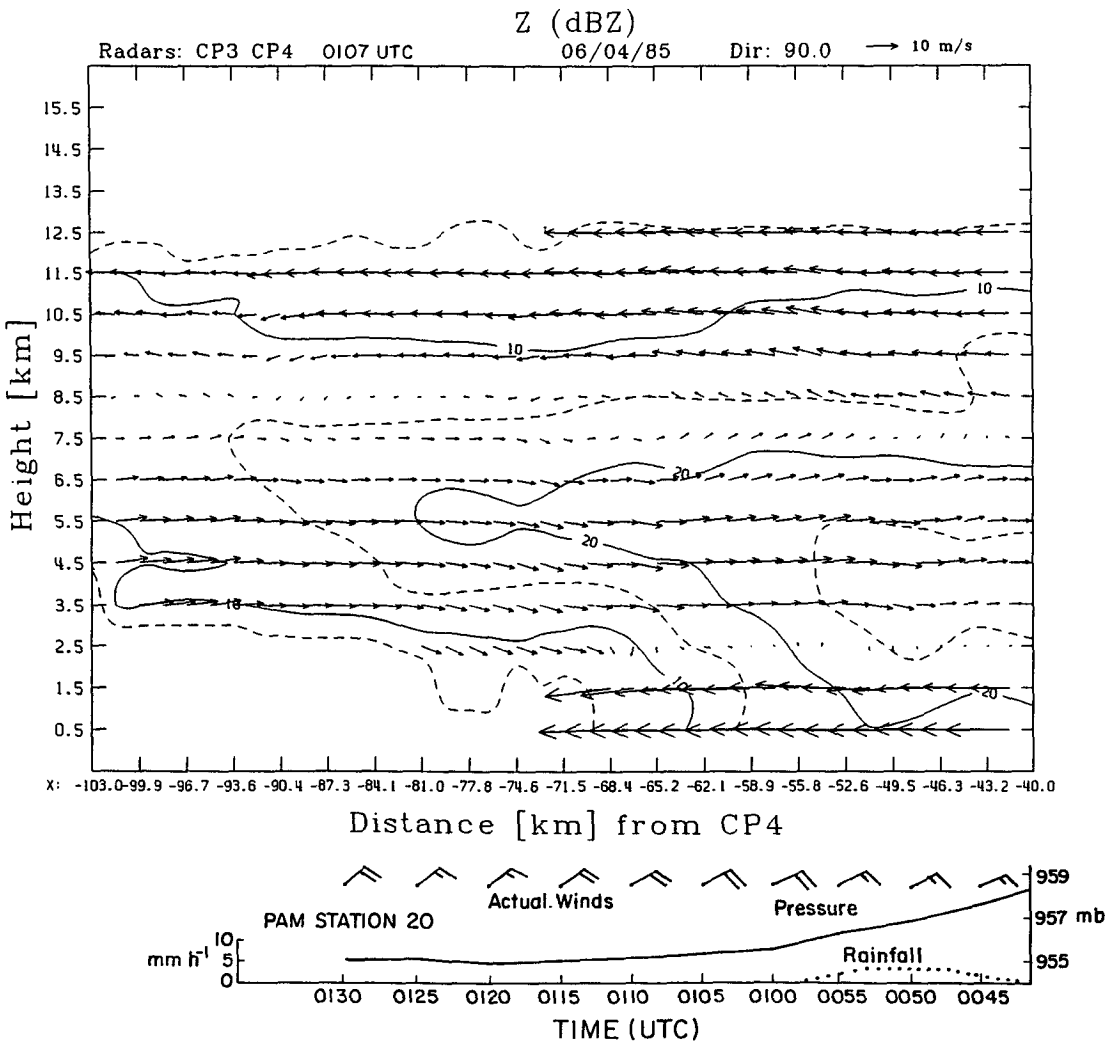

FIG. 18. As in Fig. 17, except for the E–W section 8 km north of CP-4 near PAM Station 20. Vertical motion is everywhere less than 3 m s^{-1}.

intense downdrafts and strong lower-tropospheric flow acceleration found at the back edge of the rain region near the wake low. This converse relationship also points to a linkage between locally intense subsidence at the edge of a stratiform rain area and wake-low development. Also evident from Fig. 18 is a greater eastward penetration of the rear inflow jet in the southern part of the domain toward the leading convective line (also seen in Fig. 16). This kinematic pattern is consistent with the distribution of evaporation over a broader zone in the x direction, thus, resulting in a notably weaker reflectivity gradient than seen in Fig. 17. The rapid descent of the rear inflow jet in the north (and production of an intense surface pressure gradient) occur in a portion of the trailing stratiform region containing the maximum precipitation rates (cf., rainfall rate curves in Figs. 17, 18). A similar association between trailing stratiform precipitation maxima and wake-low intensity has been noted in studies by Johnson and Hamilton (1988), Johnson et al. (1989), and Green (1989).

Additional evidence of processes unique to the wake-low region is provided in Fig. 19, which shows the area-averaged profile of vertical motion over the Doppler analysis domain (or more specifically, that part of the domain covered by detectable echo at each level). Figure 19 shows two other profiles. One (SW domain) is for the western three-quarters of an 80 km × 80 km region south of the wake low (Smull and Augustine 1989). The other, based on an EVAD analysis, is over CP-3 deep within the stratiform region (analysis developed by T. J. Matejka and computations provided to us by S. A. Rutledge). The EVAD profile displays a classic mesoscale updraft–downdraft signature. By contrast, the wake-low region and SW domain profiles are predominantly characterized by mesoscale descent over the full depth of the troposphere. (A very similar wake-low profile is obtained even if locally intense downdrafts such as those shown in Fig. 17 are excluded from the calculation.) When interpreting the EVAD analyses, it should be kept in mind that while they indicate low-level descent over a mesoscale area, the dual-Doppler analysis indicates that much of this descent is concentrated in a narrow ~10-km zone.

As noted above, a distinction between the CP-3 EVAD and wake-low domain profiles exists aloft, with the EVAD-deduced upward motion aloft suggesting the generation of stratiform precipitation in the CP-3 area. Low-level sinking occurred in both regions, but such sinking does not necessarily produce warming if melting and evaporative cooling occur. Indeed, melting and evaporation occurred at low levels over all of the CP-3 EVAD area, but only a small (<20%) portion of the wake-low domain. Thus, latent cooling offset subsidence warming in the CP-3 area and a significant pressure fall did not occur. The effect of this process on wake-low production was discussed in Johnson and Hamilton (1988) and is supported by the modeling results of Zhang and Gao (1989).

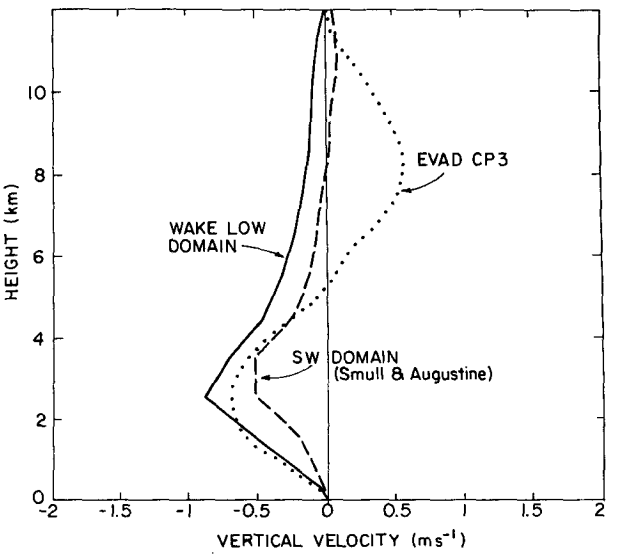

FIG. 19. Vertical motion (cm s^{-1}) over wake-low domain (solid), the western three-quarters of an 80 km × 80 km domain southwest of CP-3 and CP-4 (dashed; from Smull and Augustine 1989) and CP-3 (dotted) based on EVAD analysis (S. A. Rutledge, personal communication) at 0104 UTC 4 June 1985.

The deep layer of descent in the wake-low domain (Fig. 19) is also an indication of the descending rear inflow jet near and beneath the sloping base of the trailing stratiform cloud (Fig. 10). Sublimation likely negated some of the warming at higher levels (Johnson and Hamilton 1988, p. 1467), although weak warming still occurred between 700 and 500 mb (Fig. 12). However, because the warming aloft was less than that at low levels and the air density aloft is less, its contribution to the surface pressure reduction was small.

b. Sounding data analysis

In section 5 it was pointed out that the surface pressure fall in the wake low could be attributed to subsidence warming in the lower troposphere, as illustrated in the soundings from Russell, Kansas. This low-level warming deduced from the 0000 and 0130 soundings is depicted in greater detail in Fig. 20. It can be seen that the warming begins near 0.8 km (0.2 km AGL) and quickly reaches a maximum of 5 K near 1.0 km (0.5 km AGL). The hydrostatic pressure change (ΔP) associated with this warming is also shown in Fig. 20. Considering that ΔP at the surface is −3.5 mb and ΔP at 3.0 km is −0.6 mb, it is evident that 83% of the surface pressure fall is due to warming below 3 km (2.4 km AGL).

A further interpretation of the mechanism for lowering surface pressure involves a consideration of the

cool, stable air below the warm frontal inversion in Kansas. As strong downdrafts (Fig. 17) impact on this stable layer, there can be a local reduction in its depth and a consequent reduction in surface pressure (Bedard and LeFebvre 1986; Johnson et al. 1989). Prior to the arrival of the wake low, a warm frontal inversion extended to 1.4 km (0000 sounding in Fig. 20). Strong subsidence in the wake low depressed the top of this layer to near 1.0 km. The contribution to the surface pressure fall by this depression of the inversion, and the introduction of warm air above it (to 1.4 km), is 1.2 mb. This value represents approximately one-third of the total surface pressure fall. An indication that this inversion layer was indeed depressed, is the observation of a recovery of the frontal inversion depth to 1.5 km at Russell at 0300 (sounding not shown). This recovery is likely due to advective processes as the subsidence weakened to the rear of the storm. It is distinct from that observed over the tropical oceans (e.g., Zipser 1977) where strong surface sensible and latent heat fluxes in the wake of squall lines contribute to boundary layer recovery through mixed layer development.

7. Interpretation of results

The foregoing analysis has provided considerable detail concerning the flow in the vicinity of the wake low in a mesoscale convective system having complex convective organization. Although the organization of the 3–4 June MCS was indeed more complex than quasi-linear squall systems, a portion of that storm developed a region of trailing stratiform precipitation resembling that commonly observed to the rear of squall lines. Much like the wake lows occurring to the rear of the more linear systems (Fujita 1955; Pedgley 1962; Johnson and Hamilton 1988), a wake low was observed behind the trailing stratiform segment. The dual-Doppler radar analysis shows very rapid descent at the back edge of the trailing stratiform segment. The association of the wake low with the trailing stratiform region, and the strongest pressure gradient with the maximum reflectivity gradient at the storm's back edge, may provide evidence for the wake-low formation process.

A key feature in the process is possibly the rear inflow jet, whose existence or intensity appears to be directly related to the existence or intensity of stratiform precipitation (Smull and Houze 1987b; Johnson and Hamilton 1988; Zhang and Gao 1989). This association may be a consequence of the mechanisms producing the mesoscale pressure field which drives the jet. It is known that the vertical profile of diabatic heating in the stratiform region (heating aloft and cooling below) is such that a midlevel mesolow is produced just above the melting level (Brown 1979; Zhang and Fritsch 1988). An analysis of the geopotential height field by Stumpf (1988) and Smull and Augustine

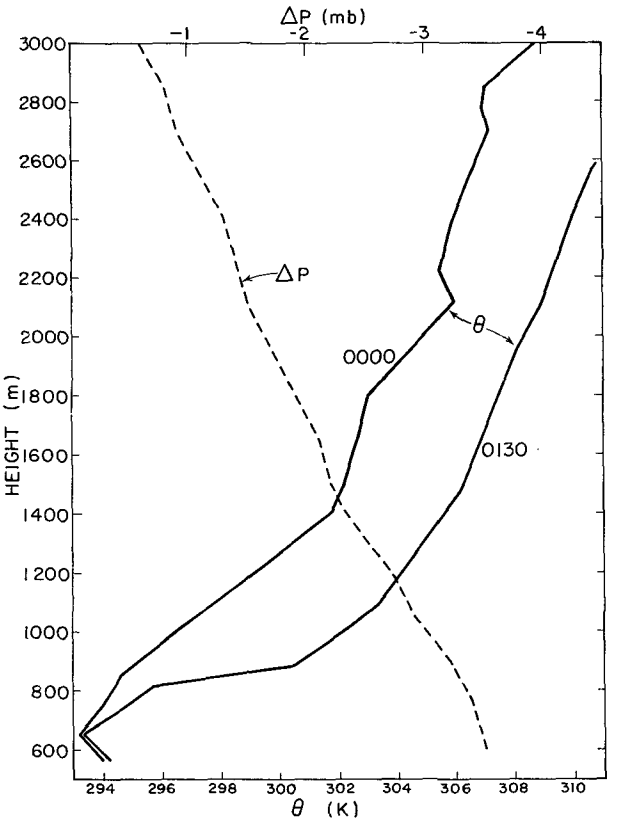

FIG. 20. Potential temperature (K) at 0000 and 0130 UTC 4 June 1985 at Russell, Kansas, (solid) and hydrostatic pressure fall (ΔP) associated with warming (dashed).

(1989) shows a perturbation low with a maximum amplitude of approximately 40 m near 550 mb (the melting level is near 620 mb) within the Kansas stratiform portion of the storm at 0000. These observations are consistent with the finding of the strongest rear-to-front flow in the northern portion (cf., Figs. 10, 13). The occurrence of the lowest pressure in the wake adjacent to the most intense stratiform rainfall (Figs. 7d, 15) may be a direct indication of a maximum rear inflow in that location and/or enhanced descent of the inflowing air driven by a maximum in melting, sublimation, and evaporation (Szeto et al. 1988).

The collocation of strongest descent with the maximum reflectivity gradient indicates strong evaporative erosion of the stratiform precipitation region by the descending rear inflow jet. With sinking motion up to 5 m s^{-1} occurring in a region of only light precipitation, significant warming can result. The obvious surface evidence of this warming is the intense pressure gradient there. The mechanism for the wake low and its tendency to "hug" the back edge of the stratiform region, as determined from this study, is therefore similar to that described in the squall line investigation of Johnson and Hamilton (1988). However, here a nar-

row zone of very strong descent in the wake-low region was detectable using dual-Doppler radar data. The descent depressed the top of the inversion by 0.4 km and this shallowing of the surface cold pool contributed up to one-third of the total surface pressure fall.

Considering the strong contrast in airmass properties across this zone of strong descent (warm, dry on one side and cool, moist on the other), this boundary in many respects resembles a mesoscale front. However, this front is decoupled from the surface due to the low-level inversion capping the outflow layer and is distinct and separated from both the density-current-driven gust front accompanying the leading convective line and the surface convergence zone to the rear of the wake low. Nevertheless, its impact on surface wind and pressure fields in this storm were just as, or even more significant than those associated with the leading gust front.

8. Summary and conclusions

An analysis has been carried out of the surface pressure field and its relationship to the cloud, precipitation, and airflow structure of a midlatitude mesoscale convective system (MCS) having complex convective organization. The MCS was the second in a sequence of four that developed over Kansas and Oklahoma on 3–4 June 1985 during the Oklahoma–Kansas Preliminary Regional Experiment for STORM-Central (OK PRESTORM). During its mature stage, the MCS consisted of two intersecting convective bands, one oriented NE–SW and the other N–S, with a stratiform region extending to the north and west of the bands. The overall precipitation structure at this time resembled that occurring in the open-wave stage of an extratropical cyclone, though on a smaller scale and in the presence of a profoundly different surface pressure pattern. Very little, if any, stratiform precipitation existed adjacent to the convective line in the southern portion of the MCS.

The primary findings of this study are twofold:

a. A wake low was observed during the mature stage of this complexly organized MCS and its position and intensity bore a striking resemblance to the well-documented wake lows occurring with quasi-linear squall systems. In particular, the lowest pressure occurred just to the rear of the trailing stratiform precipitation segment of the MCS. This portion of the storm contained a rear inflow jet (Smull and Houze 1987a,b) that descended to the lower troposphere at the position of the wake low. In the southern portion of the MCS, which did not have a trailing stratiform segment, neither a pronounced descending rear inflow jet nor a wake low was observed. This finding, in combination with those of other studies (Pedgley 1962; Zipser 1977; Johnson and Hamilton 1988; Johnson et al. 1989), strongly suggests that the trailing stratiform precipitation region of an MCS is vital for the production of a wake low. A similar conclusion has been drawn in a numerical modeling study by Zhang and Gao (1989). It is concluded that even MCSs having rather complex precipitation structures (in relation to quasi-linear squall systems) can have associated wake lows, as long as at least some portion of the storm contains a trailing stratiform segment.

b. Detailed dual-Doppler measurements indicate remarkably strong subsidence (up to 6 m s^{-1}) within the rear inflow jet in the lower troposphere and on a 10-km scale at the back edge of the trailing stratiform region near the center of the wake low. The maximum sinking occurred in the region of the strongest low-level reflectivity gradient and was coincident with the strongest surface pressure gradient adjacent to the wake-low center. In this zone, surface pressure falls up to 2.2 mb $(5\ \text{min})^{-1}$ were observed. This intense subsidence produced dramatic low-level warming and drying which created, in effect, an elevated mesoscale front at the back edge of the stratiform region. The influence of this front on surface wind and pressure changes is just as, if not more, pronounced than that associated with the MCS-leading gust front. The dual-Doppler data showed that the strongest gradients of pressure and radar reflectivity occurred to the rear of that portion of the trailing stratiform region containing the highest precipitation rate (reflectivities exceeding 35 dBZ). The strong descent also led to a local reduction in the depth of the cold air beneath a frontal inversion that existed in the region, an effect which contributed up to one-third of the surface pressure fall in the wake low. This process may be important in creating the spectacular surface pressure falls observed in instances where squall lines pass over very strong surface inversions (e.g., Bosart and Seimon 1988).

To the south of the wake-low center (in the dual-Doppler domain) the subsidence, reflectivity gradient, maximum reflectivity in the stratiform region, and surface pressure gradient were all considerably reduced. These findings further support the idea that the wake low is produced by a rapidly descending rear inflow jet to the rear of an MCS trailing stratiform precipitation region and that the low is deepest adjacent to the most intense portion of the stratiform precipitation region (Johnson and Hamilton 1988).

Evidence is accumulating to indicate that, rather than being passive debris from deep convective cells, the stratiform portions of MCSs can (under certain circumstances) be dynamically active precipitation features (Houze et al. 1989). This conclusion is drawn from the observation of intense localized rear inflow jets in the vicinity of a number of trailing stratiform regions (Smull and Houze 1987a,b; Rutledge et al. 1988), and the associated subsidence warming and intense surface pressure gradients at their back edge (Johnson and Hamilton 1988; Johnson et al. 1989 and this study). Lafore and Moncreiff (1989) also argue that the stratiform region is important in squall prop-

agation and longevity. In light of these findings, it is apparent that future field experiments should commit an important component of their resources to the measurement of stratiform and poststratiform atmospheric conditions associated with mesoscale convective systems.

Acknowledgments. The authors appreciate the assistance of John Augustine and Doug Burks with the preparation and display of mesonetwork data and thank Steve Rutledge for helpful discussions and EVAD analysis data. Thanks are also extended to Michael Fortune, Ray McAnelly, José Meitín, and James Toth for their help at various stages of the research and to an anonymous reviewer and Prof. Colleen Leary for their helpful comments on the manuscript. This research has been supported by the National Science Foundation, Atmospheric Sciences Division, under Grant ATM-8711649.

REFERENCES

Augustine, J. A., and E. J. Zipser, 1987: The use of wind profilers in a mesoscale experiment. *Bull. Amer. Meteor. Soc.*, **68,** 4–17.

——, and K. W. Howard, 1988: Mesoscale convective complexes over the United States during 1985. *Mon. Wea. Rev.*, **113,** 685–701.

Bedard, A. J., Jr., and T. T. LeFebvre, 1986: Surface measurements of gust fronts and microbursts during the JAWS Project: statistical results and implications for wind shear detection, prediction, and modeling. NOAA Tech. Memo. ERL WPL-135, 112 pp. [NTIS PB86-200847.]

Bosart, L. F., and A. Seimon, 1988: A case study of an unusually intense atmospheric gravity wave. *Mon. Wea. Rev.*, **116,** 1857–1886.

Brandes, E. A., 1990: Evolution and structure of the 6–7 May 1985 mesoscale convective system and associated vortex. *Mon. Wea. Rev.*, **118,** 109–127.

Brown, J. M., 1979: Mesoscale unsaturated downdrafts driven by rainfall evaporation: a numerical study. *J. Atmos. Sci.*, **36,** 313–338.

Cunning, J. B., 1986: The Oklahoma-Kansas Preliminary Regional Experiment for STORM-Central. *Bull. Amer. Meteor. Soc.*, **67,** 1478–1486.

Fankhauser, J. C., 1974: The derivation of consistent fields of wind and geopotential height from mesoscale rawinsonde data. *J. Appl. Meteor.*, **13,** 637–646.

Fortune, M. A., 1989: The evolution of vortical patterns and vortices in mesoscale convective complexes. Colorado State University, Atmospheric Science Paper No. 449, 183 pp. [Available from Prof. William R. Cotton at the Dept. of Atmospheric Science, Colorado State University, Fort Collins, CO, 80523.]

Fritsch, J. M., and C. G. Chappell, 1980: Numerical prediction of convectively driven mesoscale pressure systems. Part II: Mesoscale model. *J. Atmos. Sci.*, **37,** 1734–1762.

——, R. J. Kane and C. R. Chelius, 1986: The contribution of mesoscale convective weather systems to the warm-season precipitation in the United States. *J. Climate Appl. Meteor.*, **25,** 1333–1345.

Fujita, T. T., 1955: Results of detailed synoptic studies of squall lines. *Tellus*, **7,** 405–436.

Gamache, J. F., and R. A. Houze, Jr., 1982: Mesoscale air motions associated with a tropical squall line. *Mon. Wea. Rev.*, **110,** 118–135.

Garratt, J. R., and W. L. Physick, 1983: Low-level wind response to mesoscale pressure systems. *Bound.-Layer Meteor.*, **27,** 69–87.

Green, J. L., 1989: Analysis of surface pressure features during an episode of mesoscale convective systems. M.S. thesis, Texas Tech University, 75 pp. [Available from Prof. Colleen Leary, Atmospheric Science Group, Texas Tech University, Lubbock, TX, 79409.]

Houze, R. A., Jr., S. A. Rutledge, M. I. Biggerstaff and B. F. Smull, 1989: Interpretation of Doppler weather radar displays of midlatitude mesoscale convective systems. *Bull. Amer. Meteor. Soc.*, **70,** 608–619.

——, B. F. Smull and P. Dodge, 1990: Mesoscale organization of springtime rainstorms in Oklahoma. *Mon. Wea. Rev.*, **118,** 613–654.

Hoxit, L. R., C. F. Chappell and J. M. Fritsch, 1976: Formation of mesolows or pressure troughs in advance of cumulonimbus clouds. *Mon. Wea. Rev.*, **104,** 1419–1428.

Johnson, R. H., and J. J. Toth, 1986: Preliminary data quality analysis for the Oklahoma–Kansas PRE STORM PAM II mesonetwork. Colorado State University, Atmospheric Science Paper No. 407, 41 pp. [Available from the authors at the Department of Atmospheric Science, Colorado State University, Fort Collins, CO, 80523.]

——, and P. J. Hamilton, 1988: The relationship of surface pressure features to the precipitation and air flow structure of an intense midlatitude squall line. *Mon. Wea. Rev.*, **116,** 1444–1472.

——, S. Chen and J. J. Toth, 1989: Circulations associated with a mature-to-decaying midlatitude mesoscale convective system. Part I: Surface features—Heat bursts and mesolow development. *Mon. Wea. Rev.*, **117,** 942–959.

Lafore, J.-P., and M. W. Moncrieff, 1989: A numerical investigation of the organization and interaction of the convective and stratiform regions of tropical squall lines. *J. Atmos. Sci.*, **46,** 521–544.

Leary, C. A., and R. A. Houze, Jr., 1979: Melting and evaporation of hydrometeors in precipitation from the anvil clouds of deep tropical convection. *J. Atmos. Sci.*, **36,** 669–679.

——, and T. M. Bals, 1989: Evolution of the 3–4 June PRE-STORM mesoscale convective system. Preprint, *24th Conf. on Radar Meteorology,* Tallahassee, Amer. Meteor. Soc., 471–474.

Maddox, R. A., 1980: Mesoscale convective complexes. *Bull. Amer. Meteor. Soc.*, **61,** 1374–1387.

Newton, C. W., 1966: Circulations in large sheared cumulonimbus. *Tellus*, **18,** 699–713.

——, and J. C. Fankhauser, 1964: On the movements of convective storms, with emphasis on size discrimination in relation to waterbudget requirements. *J. Appl. Meteor.*, **3,** 651–688.

O'Brien, J. J., 1970: Alternative solutions to the classical vertical velocity problem. *J. Appl. Meteor.*, **9,** 197–203.

Pedgley, D. E., 1962: A mesosynoptic analysis of the thunderstorms on 28 August 1958. *Brit. Meteor. Off. Geophys. Mem.*, **106,** 74 pp.

Rutledge, S. A., R. A. Houze, Jr., M. I. Biggerstaff and T. Matejka, 1988: The Oklahoma–Kansas mesoscale convective system of 10–11 June 1985: precipitation structure and single-Doppler radar analysis. *Mon. Wea. Rev.*, **116,** 1409–1430.

Smull, B. F., and R. A. Houze, Jr., 1985: A midlatitude squall line with a trailing region of stratiform rain: radar and satellite observations. *Mon. Wea. Rev.*, **113,** 117–133.

——, and ——, 1987a: Dual-Doppler radar analysis of a midlatitude squall line with a trailing region of stratiform rain. *J. Atmos. Sci.*, **44,** 2128–2148.

——, and ——, 1987b: Rear inflow in squall lines with trailing stratiform precipitation. *Mon. Wea. Rev.*, **115,** 2869–2889.

——, and J. A. Augustine, 1989: Structure and environment of a nonsquall mesoscale convective complex observed during PRESTORM. Preprints, *24th Conf. on Radar Meteorology,* Tallahassee, Amer. Meteor. Soc., 502–504.

——, and D. P. Jorgensen, 1990: Pressure and buoyancy perturbations near an intense wake low in a midlatitude mesoscale convective system. *Extended Abstracts, 4th Conf. on Mesoscale Processes,* Boulder, Amer. Meteor. Soc., 214–215.

Srivastava, R. C., T. J. Matejka and T. J. Lorello, 1986: Doppler radar study of the trailing anvil region associated with a squall line. *J. Atmos. Sci.*, **43,** 356–377.

Stumpf, G. J., 1988: Surface pressure features associated with a mid-latitude mesoscale convective system in OK PRE-STORM. CSU Dept. of Atmospheric Science Paper No. 435, 148 pp. [Available from Prof. Richard H. Johnson at Dept. of Atmospheric Science, Colorado State University, Fort Collins, CO, 80523.]

——, and R. H. Johnson, 1988: Lower tropospheric profiling needs in relation to the initiation of mesoscale convective systems. Preprints, *Symp. on Lower Tropospheric Profiling: Needs and Technologies,* Boulder, Amer. Meteor. Soc., 29–30.

Szeto, K. K., R. E. Stewart and C. A. Lin, 1988: Mesoscale circulations forced by melting snow. Part II: Application to meteorological features. *J. Atmos. Sci.*, **45,** 1642–1650.

Williams, D. T., 1954: A surface study of a depression-type pressure wave. *Mon. Wea. Rev.*, **82,** 289–295.

——, 1963: The thunderstorm wake of 4 May, 1961. Natl. Severe Storms Project Rep. No. 18, U.S. Dept. of Commerce, Washington DC, 23 pp. [NTIS PB 168223.]

Zhang, D.-L., and J. M. Fritsch, 1988: A numerical investigation of a convectively generated, inertially stable, extratropical warm-core mesovortex over land. Part I: Structure and evolution. *Mon. Wea. Rev.*, **116,** 2660–2687.

——, and K. Gao, 1989: Numerical simulation of intense squall line during 10–11 June 1985 PRE-STORM. Part II: Rear inflow, surface pressure perturbations and stratiform precipitation. *Mon. Wea. Rev.*, **117,** 2067–2094.

——, —— and D. B. Parsons, 1989: Numerical simulation of an intense squall line during 10–11 June 1985 PRE-STORM. Part I: Model verification. *Mon. Wea. Rev.*, **117,** 960–994.

Zipser, 1977: Mesoscale and convective-scale downdrafts as distinct components of squall-line circulation. *Mon. Wea. Rev.*, **105,** 1568–1589.